

Master Degree course in Automotive Engineering

Master Degree Thesis

ABS Control System Design for Electric Bikes Based on Wheel Acceleration: A Conjugate Boundary and Genetic Algorithm Approach

Supervisors

Prof. ANDREA TONOLI

Prof. LUIS MIGUEL CASTELLANOS MOLINA

Candidate ZHANG HENGYU

ACADEMIC YEAR 2024-2025

Abstract

This thesis aims to design a high-performance anti-lock braking control system for electric bikes to enhance rider safety and improve the maneuverability of bikes under various road conditions, addressing a significant gap in low-cost active safety solutions for this rapidly growing mode of transportation. A conjugate boundary method is used as the control strategy, which offers the distinct advantage of relying only on wheel acceleration data, thereby eliminating the need for expensive vehicle speed or inertial measurement sensors. A simulation model of the E-bike, integrating both longitudinal and vertical dynamics, was developed in MATLAB/Simulink to represent braking behavior. To overcome the challenge of tuning the CBM's parameters, a Genetic Algorithm (GA) was employed to automatically optimize the controller. The simulation results demonstrate the effectiveness and robustness of the designed control system across a range of conditions, including dry, wet, snowy, and icy roads. This approach provides a practical solution for E-bikes that lack advanced sensors. In future work, the proposed ABS control system will be integrated into a real commercial electric bike to enhance performance and safety.

Contents

1	Introduction			3		
2	System model 6					
	2.1	Bike n	nodel	6		
	2.2	Road	profile	13		
	2.3	Tire m	nodel	14		
	2.4		al dynamic model	16		
	2.5		system	16		
	2.6		limitations and critical analysis	24		
		2.6.1	Limitations of the Bike Model	24		
		2.6.2	Limitations of the Tire Model	24		
		2.6.3	Limitations of the Braking System Model	25		
		2.6.4	Conclusion on Limitations	$\frac{1}{25}$		
	2.7		Parameters Summary	25		
3	Nur	nerical	l evaluation	27		
		3.0.1	Overall control strategy	27		
	3.1	Metho	odology	27		
		3.1.1	Conjugate boundary method controller design	27		
		3.1.2	Parameters optimization via Genetic Algorithm	30		
	3.2	Simula	ation scheme used for GA	32		
	3.3					
		3.3.1	Dry road simulation result	34 34		
		3.3.2	Wet road simulation result	37		
		3.3.3	Snow road simulation result	40		
		3.3.4	Ice road simulation result	43		
		3.3.5	Summary of Results	45		
				4.0		
4	Con	clusio		46		
		4.0.1	Future work	46		
Re	efere	nces		48		

Chapter 1

Introduction

Nowadays, as European cities continue to grow and urban populations expand, urban transportation faces significant challenges, with congestion and accidents becoming increasingly common. People are encouraged to walk and cycle more. New modes of transportation are constantly emerging, including electric bikes.

Electric bikes (E-bikes) offer low cost, convenience, and zero emissions compared to traditional fuel-based vehicles. They help improve the environment, ease last-mile access, reduce urban congestion, and lower travel costs. Due to these driving factors, the global E-bike market has experienced double-digit growth rates. The market is projected to grow from \$50.14 billion in 2024 to \$148.70 billion by 2032, exhibiting a CAGR of 14.6% during the forecast period, and possesses great market potential [1].

However, the average speed and weight of E-bikes are higher than those of ordinary bicycles. Their increasing popularity has brought new safety challenges. The increased kinetic energy means longer braking distances and a higher risk of losing control during emergency maneuvers.

According to European Transport Safety Council (ETSC) reports, statistics in urban centers are stark [2]: 70% of reported road fatalities involve pedestrians, cyclists, and powered two-wheeler (PTW) riders. Compared to motor vehicles, vulnerable road users such as cyclists face an extremely high risk of injury in collisions.

An in-depth accident analysis by the German Accident Research Institute indicates that 'loss of vehicle control' is a primary cause in single-vehicle accidents resulting in serious injuries [3].

From the viewpoint of vehicle dynamics, during emergency braking conditions, wheel lockup is the most direct cause of loss of control, primarily due to skidding and rollover. The most common solution is applying Anti-lock Braking Systems (ABS). Many studies prove that ABS can reduce braking distance and reduce accidents [4] [5]. It helps the wheels keep rotating slightly to avoid lockup while hard braking. This can ensure that the vehicle always has sufficient braking force and maneuverability. However, the application of anti-lock braking systems remains far from popular in the E-bike sector, and there is a significant research gap in this area. Academic research focuses on algorithm optimization and low-cost solutions, demonstrating that existing approaches are not perfect [5] [6]. This has resulted in E-bikes equipped with ABS not being widely sold on the market. As of

2025, bicycles equipped with ABS (primarily E-Bikes) account for a negligible share of global bicycle sales(The global market, valued at approximately \$250 million in 2025 for ABS E-bikes Vs 77.01 billion for bicycles). It remains a "high-end" or even "conceptual" feature, far from becoming a necessity as it has in automobiles [7]. Therefore, developing an efficient, low-cost E-bike ABS control system has significant practical importance and market influence for limiting loss of control during emergency braking and enhancing active safety.

Nevertheless, it is crucial to highlight the fundamental differences between an ABS on a car and on a bicycle. Car ABS utilizes a complex system of wheel speed sensors and an Electronic Control Unit (ECU) to monitor and adjust brake pressure to each wheel individually. When the driver depresses the brake pedal, the ABS ECU commands a booster–pump hydraulic unit to actively increase, hold, or decrease brake pressure and regulates wheel slip toward a target slip ratio using multi-channel valves plus an accumulator–pump pair. However, for bicycle ABS, the master pressure level is determined by the rider, and the rate is limited. The adjustable braking pressure of the ABS cannot exceed the pressure applied by the rider on the master lever. This difference directly dictates the accumulator sizing. A car requires a large volume accumulator to handle the fluid discharged from four large calipers during pressure release cycles. Conversely, a bicycle ABS, typically controlling only the front wheel, requires only a small accumulation chamber. Such differences constrain the performance of bicycle ABS, thereby presenting greater challenges in the design of ABS control systems.

So, in this thesis, a high-performance and low-cost ABS control system for E-bikes is designed that only relies on wheel speed sensors and wheel acceleration data. It is simple and does not need expensive sensors. Its purpose is to shorten braking distances and enhance maneuverability under varying road conditions.

The primary contribution of this thesis is to use a proposed control method called the Conjugate Boundary Method (CBM) to modulate brake pressure [5] [8]. The core principle of the CBM is to use only wheel acceleration data to determine when to increase or release brake pressure, eliminating the need for a vehicle velocity sensor to calculate the slip ratio. A Genetic Algorithm (GA) is employed to automatically optimize the CBM's control parameters, ensuring minimal braking distance across diverse road conditions [9]. The proposed system is comprehensively simulated and tested within a MATLAB/Simulink environment to verify its efficacy.

In short, this thesis is divided into four chapters:

- Chapter 1 Introduction: This chapter outlines the background for designing an ABS control system for e-bikes, demonstrating the motivation for the design from the aspects of market gaps, market potential, and research gaps. It also highlights the differences between ABS systems on bicycles and those on automobiles.
- Chapter 2 System Model: This chapter presents a mathematical model for electric bicycles designed for ABS systems. Content covers bike dynamics, road profiles, tire models, vertical dynamics, and braking systems. The model integrates longitudinal and vertical motion, capturing effects such as load transfer and road surface irregularities. Simplifications and assumptions are discussed, with particular emphasis

on the model's applicability and limitations. Specific values for all parameters are listed at the chapter's conclusion to facilitate simulation result replication.

- Chapter 3 Methodology & Simulation results: This chapter provides a detailed explanation of the control strategy for designing an ABS control system: the Conjugate Boundary Method. It also provides a detailed introduction to its parameter tuning method: the genetic algorithm. Simulate braking with and without ABS in MATLAB to obtain results for different road conditions.
- Chapter 4 Conclusion: The final chapter summarizes the research contributions, emphasizing the effectiveness of the proposed low-cost ABS control system based on CBM and GA optimization. It highlights the improvements in braking safety and stability, while also pointing out the need for real-world validation. Future work will focus on simulating more complex, realistic models (adding accumulators and restore phases to the braking system, incorporating rollover motion and skidding into bike dynamics), and ultimately applying the designed ABS control system to actual commercial E-bikes.

Chapter 2

System model

This chapter introduces the electric bike model, tire model, vertical dynamic model, and brake system used in ABS control system design. The goal is to provide a background to understand how the E-bike behaves during braking. The E-bike is modeled as a longitudinal dynamic system with vertical suspension, neglecting air drag. It is also integrated with road profile interaction, and the braking performance is tested under an urban road profile. By adjusting the parameters of the Pacejka Magic Formula, the model can also be tested under different road friction levels.

2.1 Bike model

Before establishing the dynamic model of an E-bike, in order to focus on the core research issue of the anti-lock braking system (ABS): the longitudinal dynamics of the tire-road contact surface, and reduce the complexity of the model, this paper neglects aerodynamic resistance. The speed of electric bicycles is relatively low with respect to vehicle speed. The deceleration force generated by air resistance is smaller in magnitude compared to the braking force produced by the mechanical braking system. Therefore, neglecting air drag will not have a significant impact on the longitudinal dynamic simulation results under emergency braking conditions, and it can also simplify the state equation and improve the computational efficiency.



Figure 2.1. E-bike

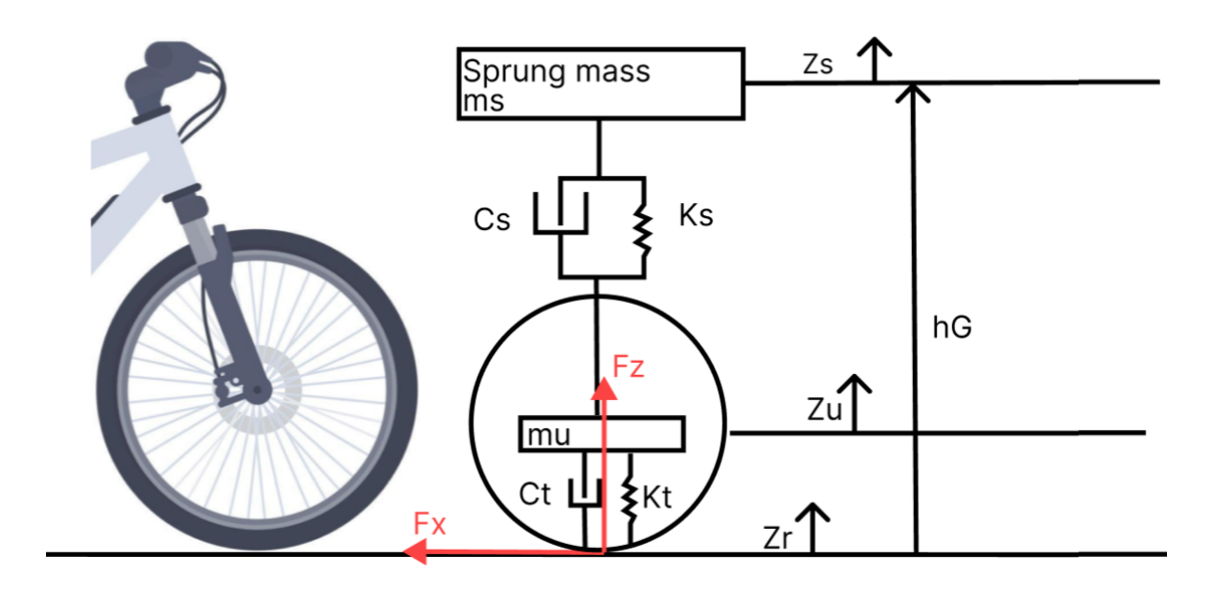


Figure 2.2. Bike model

A longitudinal single-wheel model integrated with vertical dynamics is used in this study, which is constructed based on the framework of the quarter car model. The choice was based on the following considerations:

• The core function of ABS is to manage the longitudinal force at the tire-road interface. Therefore, a single-wheel longitudinal model that accurately reflects the

relationship between slip ratio κ , wheel speed ω , and vehicle speed v_x constitutes a sufficient starting point.

- However, the longitudinal force generated by the tire is highly dependent on its vertical load F_z . This load is not constant during actual braking; it varies dynamically due to load transfer and road profile. To capture this crucial physical phenomenon, this model introduces the vertical dynamics component of a quarter vehicle model, which includes the sprung mass M_s , unsprung mass M_u , suspension stiffness K_s , and damping C_s .
- Therefore, the model established in this paper can simulate both the static load transfer induced by deceleration during braking (2.8) and the dynamic load variations caused by road profile (2.14). This allows the tire's vertical load F_{z_total} to become a dynamic state variable, significantly enhancing the fidelity of braking behavior simulations under complex road conditions. This approach is better than traditional single-wheel models that assume a constant vertical load.

In conclusion, this model is an extended single-wheel model for longitudinal braking analysis that considers vertical dynamic loads. Additionally, to simulate the braking process of an e-bike, the model requires integration of a braking system where the caliper provides braking torque. This torque is generated by pressure within the brake caliper; hence, the model state must also include caliper pressure.

More specifically, to accurately capture the dynamic behavior of E-bikes during braking and preserve variables directly relevant to ABS controller design, this study selected 9 state variables for the model (2.1). Position x, longitudinal velocity v_x , wheel angular velocity ω , displacement of sprung mass Z_s displacement of unsprung mass Z_u , velocity of sprung mass v_s , velocity of unsprung mass v_s , longitudinal slip ratio κ , and caliper pressure P_{caliper} .

Among these states, v_x , ω and κ are the necessary kinematic quantities for achieving the coupling of braking and tire mechanics, to describe the relationship between the tire's longitudinal force and slip. And introduce vertical dynamics, Z_s , Z_u , v_s , v_u , enabling the vertical load F_{z_total} to function as a dynamic variable reflecting instantaneous load variations caused by road surface irregularities, thereby directly influencing the Pacejka longitudinal force F_x . Finally, applying caliper pressure P_{caliper} reflects the dynamics of the hydraulic system (the rate of pressure rise/release relative to valve limitations), which is a key limiting factor for the performance of ABS implementation and control strategies. In summary, these 9 states provide a sufficiently clear description of the bicycle's state of motion without being too complex, which can be a crucial foundation for future ABS design.

Thus, the dynamics of the E-bike are defined by a state-space representation with a 9-dimensional state vector:

$$\xi = \left[x, v_x, \omega, Z_s, Z_u, v_s, v_u, \kappa, P_{\text{caliper}}, \right]^T$$
(2.1)

Where each state represents a physical quantity in the system:

• x: Position of the bike

- v_x : Velocity of the bike
- ω : Angular speed of the wheel
- Z_s : Displacement of the sprung mass
- Z_u : Displacement of the unsprung mass
- v_s : Vertical velocity of the sprung mass
- v_u : Vertical velocity of the unsprung mass
- κ: Slip ratio
- P_{caliper} : Caliper pressure

The system is driven by a 4-dimensional input vector \mathbf{U} , which includes all external forces and commands acting on the model:

$$\mathbf{U} = \begin{bmatrix} P_{\text{master}}, \ P_{\text{cCMD}}, \ F_{\text{traction}}, \ Z_{\text{road}} \end{bmatrix}^T$$
 (2.2)

Each element of U represents a distinct external influence:

- P_{master} : Pressure on the master brake lever applied by the rider. This variable represents the rider's braking intent. When the rider wants to brake urgently, the brake lever is pressed down rapidly, generating P_{master} .
- P_{cCMD} : Commanded pressure at the caliper from the ABS controller. This is a control signal from the ABS controller to the hydraulic modulator (solenoid valves). It adjusts the caliper pressure by opening or closing the hold/release valves.
- F_{traction} : Traction force applied to the bike. It is zero while braking. Although traction force is set to zero during braking maneuvers, it is included in the model for generality and to allow extension to combined driving—braking scenarios.
- Z_{road}: Road profile excitation. This input introduces the effect of the road surface
 on the vertical dynamics. It acts as an external disturbance transmitted through
 the suspension and tire stiffness, generating variations in the vertical load F_{z_road}.
 These fluctuations have a direct influence on the tire-road friction force; this external disturbance makes the simulation more realistic compared to models with
 constant normal load.

The evolution of the state vector ξ is governed by a set of nonlinear ordinary differential

equations of the form $\dot{\xi} = f(\xi, \{U\})$, which are derived in the following:

$$\begin{split} \dot{\xi} &= [V_x \\ &\frac{1}{m} \left(F_x + F_{\text{traction}} \right) \\ &\frac{1}{J_\omega} \left(-b_r \omega - \left(F_x R_{\text{wheel}} + M_r \right) + T_{\text{brake}} \tanh(-\omega) \right) \\ &V_s \\ &V_u \\ &\frac{1}{M_s} \left(-C_s \left(V_s - V_u \right) - k_s \left(Z_s - Z_u \right) - \Delta F_z \right) \\ &\frac{1}{M_u} \left(C_s \left(V_s - V_u \right) + k_s \left(Z_s - Z_u \right) - k_t \left(Z_u - Z_r \right) \right) \\ &\frac{1}{\tau_{\text{rel}}} \left(-k_{\text{rel}} + \kappa \right) \\ &\dot{p}_{\text{caliper}}] \end{split}$$

Among these equations, the longitudinal acceleration of the bike and the angular acceleration of the wheel are defined as follows:

$$\dot{v}_x = \frac{1}{m} \cdot (F_x + F_{\text{traction}}) \tag{2.3}$$

$$\dot{\omega} = \frac{1}{J_{\omega}} \left(-b_r \omega - (F_x R_{\text{wheel}} + M_r) + T_{\text{brake}} \tanh(-\omega) \right)$$
 (2.4)

where:

- \dot{v}_x : Longitudinal acceleration of the vehicle, calculated according to Newton's second law, and determined by the tire force and external traction force.
- m: Total mass of the rider and the bike
- F_x : Longitudinal tire force generated at the tire-road interface.
- F_{traction} : Traction force. This term is set to zero during braking in this study; however, it allows future extension to combined traction—braking conditions.
- $\dot{\omega}$: Angular acceleration of the wheel, describing the rotational dynamics during braking.
- J_w : Rotational inertia of the wheel, which determines how quickly the wheel can decelerate in response to braking torque.
- R_{wheel} : Effective radius of wheel
- b_r : Axle viscous damping coefficient, representing mechanical losses in the hub and bearings.

- M_r : Rolling friction torque, consider the energy dissipation due to tire deformation and contact with the road surface.
- T_{brake} : Braking torque generated by the caliper Note that the T_{brake} is multiplied by $\tanh(-\omega)$ to smooth the braking torque, ensuring the correct direction of the braking torque and enhancing the stability of numerical calculations. Despite the smoothing function $\tanh(-\omega)$ being a numerical approximation that improves simulation stability, it introduces slight deviations compared to real torque behavior near zero wheel speed.

The vertical dynamics of the sprung and unsprung masses are modeled as a quarter-vehicle with road profile excitation z_r , using absolute coordinates and taking displacements with respect to the static equilibrium. The acceleration of sprung and unsprung mass can be expressed as:

$$\dot{v}_s = \frac{1}{m_c} \left[-K_s(z_s - z_u) - C_s(\dot{z}_s - \dot{z}_u) - \Delta F_z \right]$$
 (2.5)

$$\dot{v}_u = \frac{1}{m_u} \left[K_s(z_s - z_u) + C_s(\dot{z}_s - \dot{z}_u) - K_t(z_u - z_r) \right]$$
 (2.6)

where: $v_s = \dot{z}_s, v_u = \dot{z}_u$ The physical meaning of each term:

- m_s , m_u are the sprung mass and unsprung mass.
- K_s , K_t are assumed linear spring suspension and tire stiffness. C_s is the linear viscous damping. However, geometric nonlinearities and tire damping are neglected.
- $K_s(z_s z_u)$ and $C_s(\dot{z}_s \dot{z}_u)$ are the spring and damping force transmitted between the body and wheel.
- $K_t(z_u z_r)$ is the tire vertical force caused by tire deflection. The tire deflection is generated by the roughness of the road surface
- ΔF_z is the load transfer. In the kinetic state, the pitch motion occurs during bike braking, resulting in a load transfer from the rear to the front axle. It is defined as $\Delta F_z = \frac{h_G \cdot m \cdot a_x}{L}$ (2.8).

Because a single-wheel (front) model is used in this study, the load distribution on the front axle must be taken into account in the static state. The load distribution is defined as:

$$F_{z0} = m \cdot g \cdot \lambda \tag{2.7}$$

Where m is the total mass (bike+rider), g the gravitational acceleration, and $\lambda \in (0,1)$ the front static weight fraction measured at rest.

During braking, the E-bike has pitch motion, and an additional quasi-static load is transferred from the rear to the front. The load transfer is defined as:

$$\Delta F_z = \frac{h_G \cdot m \cdot a_x}{L} \tag{2.8}$$

with h_G the center of gravity height and L the wheelbase. This study simulates the effects of pitch motion by using quasi-static ΔF_z rather than explicit pitch angle. This approach

is accurate for the low-speed, short-duration braking simulations under consideration. Not only reduces model complexity, but it also maintains the model's accuracy in ABS control design.

The longitudinal slip ratio κ , is a dimensionless state variable that quantifies the relative difference between the translational velocity of the wheel hub v_x and the tangential velocity of the wheel ωR_{wheel} . It is the fundamental input to the tire model (Pacejka Magic Formula in Section ??), as it directly governs the longitudinal force F_x generated at the tire-road contact patch.

The definition of the braking slip ratio is given by:

$$\kappa = \frac{\omega R_{\text{wheel}} - v_x}{v_x} \tag{2.9}$$

- During braking $(v_x > \omega R_{\text{wheel}})$: The wheel rotates slower than the vehicle, resulting in a negative slip ratio $(\kappa < 0)$. A value of $\kappa = -1$ indicates a fully locked wheel $(\omega = 0)$.
- During driving ($\omega R_{\text{wheel}} > v_x$): The wheel rotates faster than the vehicle (e.g., under motor acceleration), resulting in a positive slip ratio ($\kappa > 0$).

Note that this equation cannot be divided by zero. However, during braking, the bike's speed decreases to zero, which can cause computational errors. Therefore, this study stops the simulation when the vehicle speed falls below 8 km/h to prevent the program from reporting errors.

Additionally, the derivative of the slip ratio is defined as:

$$\frac{d\kappa}{dt} = \frac{1}{\tau_{\rm rel}} \left(-\kappa_{\rm rel} + \kappa \right) \tag{2.10}$$

where:

• $\tau_{\rm rel}$: Relaxation time constant

$$\tau_{\rm rel} = \frac{L_{\rm rel}}{\omega R_{\rm wheel}}$$
 Lrel is relaxation length of tire (2.11)

• $\kappa_{\rm rel}$: Current real slip ratio

It is essential to introduce relaxation time and relaxation length at this point. Because the longitudinal force generated by the tire does not react instantaneously to a change in the kinematic slip. Shear strain has to build up through the visco-elastic tread and along the finite contact patch; the effective slip that produces force behaves as a small lag. The absence of lag will exaggerate the actual capabilities of ABS, leading to unrealistic oscillations or 'instantaneous' force jumps. This has a negative impact on ABS control system design, as the resulting ABS may fail in real-world scenarios.

2.2 Road profile

Roads in real-world driving scenarios are not perfectly smooth. They contain irregularities that excite the vertical dynamics of the vehicle, which in turn affect the tire-road contact forces. To simulate the effect of surface irregularities on braking performance, this study employs the ISO 8608 international standard [10] to generate the road elevation profile Z_r . This selection is based on several key reasons that enhance simulation effectiveness and robustness.

First, ISO 8608 provides a standardized, quantitative framework for classifying road roughness. By using a well-defined 'Class A-F road', the results of this study can be directly compared, reproduced, and benchmarked against future or previous work by other researchers.

Second, the ISO 8608 model, based on Power Spectral Density (PSD), effectively captures the statistical properties of actual road surfaces. Introducing this level of realism is crucial for evaluating the performance of ABS controllers in environments. It simulates actual operating conditions as closely as possible, so that they can test their robustness against disturbances beyond an ideal flat road.

The road roughness is defined by a power spectral density (PSD) model, where each road class (A to F) corresponds to a specific reference PSD value at a spatial frequency $q_0 = 0.1 \,\text{cycles/m}$. The PSD decays with frequency according to a waviness exponent w = 2, following the relation:

$$PSD = PSD_0 \left(\frac{q}{q_0}\right)^{-w} \tag{2.12}$$

Where:

- PSD: Power spectral density at spatial frequency q [m³]
- PSD_0 : Reference PSD values at frequency $q_0 = 0.1 \, \text{cycles/m}$ are defined by road classes A-F
- q: Spatial frequency [cycles/m]
- w: Waviness factor, typically set to 2

The ISO 8608 classification defines road classes from A to F based on increasing levels of surface roughness, as shown in Table 2.1.

Road Class	Description	Reference PSD[m ³]
A	Very smooth highway	16×10^{-6}
В	Smooth asphalt road	64×10^{-6}
\mathbf{C}	Normal rural road	256×10^{-6}
D	Rough road	1024×10^{-6}
\mathbf{E}	Severely damaged road	4096×10^{-6}
\mathbf{F}	Off-road/very bumpy	16384×10^{-6}

Table 2.1. ISO 8608 Road Classes and Corresponding PSD Reference Values

Random phase angles are assigned to each frequency component, and an inverse Fourier transform is applied to generate the spatial profile. The result is a road height signal $Z_r(x)$, which is normalized to match the expected RMS values for each road class, ranging from very smooth highways (Class A) to extremely rough off-road surfaces (Class F). This profile is used as an input to the vertical dynamics model. As shown in Figure 2.3, there is a road profile of class A generated by MATLAB. This study focuses solely on designing an ABS for e-bikes driving on urban roads(class A); consequently, all subsequent simulations are based on urban road conditions.



Figure 2.3. Road profile(Class A)

2.3 Tire model

The Pacejka Magic Formula tire model [11]. is selected for this study to characterize the relationship between longitudinal slip ratio κ and the resulting longitudinal force F_x . This choice is based on the empirical accuracy and wide acceptance of the Pacejka model.

The Magic Formula is not a physical model derived from principles but a highly accurate empirical model. Moreover, this model effectively captures the nonlinear characteristics of the tire force-slip relationship, including the linear region at low slip, the peak friction value, and the subsequent friction decline trend at high slip. This entire curve (Figure 2.6) is important for ABS development, because the controller's goal is to maintain operation near the peak value. The parameters in this formula (B, C, D, E) have distinct definitions, such as D representing peak values and C controlling curve shape. This enables intuitive manual parameter adjustment to simulate different road surfaces (dry, wet, snow). Last but not least, compared to complex physical tire models, this model is far simpler to calculate, which is a key advantage for research requiring a large number of simulation computations.

Here is the definition of the Pacejka Magic Formula tire model:

$$F_x = F_{z \ total} \cdot D \cdot \sin\left(C \cdot \arctan\left(B \cdot \kappa - E \cdot (B \cdot \kappa - \arctan(B \cdot \kappa))\right)\right) \tag{2.13}$$

Where:

- F_x : Longitudinal tire force
- F_{z_total} : Total normal load on the tire
- κ : Longitudinal slip ratio
- B, C, D, E: Empirical Pacejka coefficients (stiffness, shape, peak, curvature)

The longitudinal tire force F_x is modeled using the Magic Formula proposed by Pacejka. It relates the slip ratio κ to the generated longitudinal force through empirical parameters B,C,D,E. These parameters respectively define the stiffness, shape, peak, and curvature of the force-slip curve, and are tuned based on road surface conditions. In this model, the Pacejka coefficients are defined as:

Parameter	Dry	Wet	Snow	Ice
\overline{B}	10	9	5	4
C	1.9	2.3	2	2
D	1.0	0.82	0.3	0.1
E	0.97	1.0	1.0	1.0

Table 2.2. Pacejka coefficients for different road conditions

These parameters, shown in Table 2.2 are selected based on typical ranges reported in the Tyre and Vehicle Dynamics by Pacejka [11]. They are also consistent with values adopted in various simulation studies for longitudinal tire dynamics under different road conditions (e.g., dry, wet, snow, ice). In this thesis, they are manually tuned within these ranges to match expected braking behavior and ensure stable ABS performance across multiple road types.

2.4 Vertical dynamic model

The vertical dynamics model consists of a tire model and a suspension system, which converts the road profile into vertical forces acting on the bike. The vertical force caused by the road profile is defined as:

$$F_{z \quad road} = k_t \cdot (Z_u - Z_r) \tag{2.14}$$

where:

- F_{z-road} : Vertical force transmitted from the road to the unsprung mass
- k_t : Tire stiffness
- Z_u : Vertical displacement of the unsprung mass
- Z_r : Vertical displacement of the road surface

Based on the road profile and tire response, the instantaneous normal load applied to the tire can be expressed as follows:

$$F_{z_total} = F_{z0} + F_{z_road} \tag{2.15}$$

Thus, the variations in vertical force caused by the road profile have been taken into

Now, the E-bike model integrates the road profile model, vertical dynamic model, and Pacejka Magic model. The input road profile Z_r is processed through the vertical dynamic model, which computes the resulting vertical load F_z on the tire. This load is then passed to the Pacejka tire model to calculate the longitudinal force F_x , which directly affects the braking behavior of the electric bike. This structure enables the simulation to account for variations in road conditions and their influence on braking performance.

2.5 Brake system

The brake system converts the input command from the rider and the ABS controller into a braking torque applied to the wheel. This system consists of a master brake lever, a hydraulic circuit, a hold valve, a release valve, an accumulator, brake pads, and brake discs, as shown in Figure 2.4. When the rider presses the master brake lever, the hydraulic system generates pressure. The hold valve normally opens. The hydraulic oil flows through the hold valve and generates pressure. This pressure pushes the pistons inside the caliper, forcing the brake pads to press against the brake discs. As a result, a brake torque is applied to the wheel.

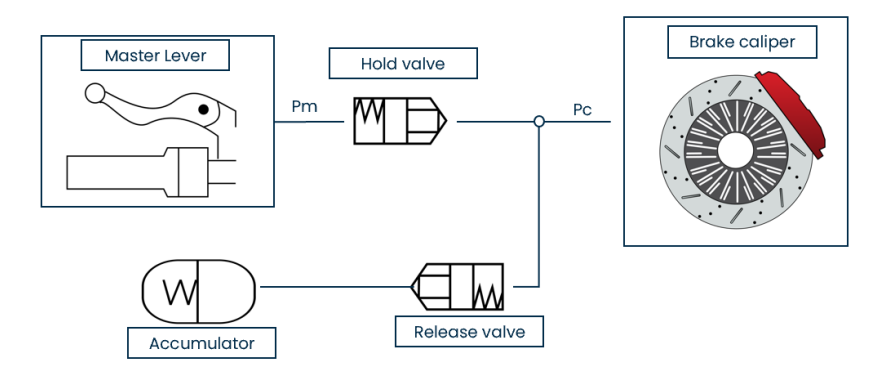


Figure 2.4. Brake system

In this model, the braking torque T_{brake} applied to the wheel is a function of the caliper pressure P_{caliper} and fundamental physical parameters of the brake system:

$$T_{\text{brake}} = 10^5 \cdot \mu \cdot P_{\text{caliper}} \cdot \pi \cdot B_a^2 \cdot R_m \cdot N_{\text{pads}}/4$$
 (2.16)

where:

- T_{brake} : The braking torque applied to the wheel
- μ : Friction coefficient between the brake pad and the disc; however, this parameter is modeled as constant, while in reality it varies with temperature fade, which is not accounted for in this study.
- P_{caliper} : Caliper pressure
- B_a : Piston radius
- R_m : Mean effective braking radius on the disc
- $N_{\rm pads}$: Number of brake pads
- 10⁵: Unit conversion factor from bar to Pascal

The core function of the ABS is to modulate the caliper pressure P_{caliper} , which is the primary state variable governing the braking process. The ABS function is implemented by controlling the opening and closing of a hydraulic solenoid valve. The valves have the following states:

- The bike is under normal braking conditions: the hold valve is kept open. The release valve is normally closed.
- Wheel lock-up is detected: the hold valve closes, and the release valve opens to release pressure by allowing the hydraulic oil to flow into the accumulator.
- Pressure reconstruction is needed: the hold valve opens again to increase pressure.

These valve states are selected by control signals from the ABS controller. When a command is sent, the hold valve switches between open and closed states, resulting in an increase or a release of caliper pressure. However, the pressure variation is not instantaneous. Due to physical and mechanical limitations, the pressure increases and decreases gradually. This variation rate has a significant influence on ABS performance. Therefore, it is necessary to properly define the variation rate of caliper pressure change in the model.

Define the variation rate of caliper pressure: On/off control(Bang-bang control) approach

The caliper pressure variation rate \dot{P}_c is a critical parameter that directly influences ABS performance. An excessively slow rate would fail to prevent wheel lock-up promptly, while an excessively fast rate could cause pressure oscillations and system instability.

In order to determine a realistic and effective value, a Bang-Bang controller was employed as a dedicated tuning tool. The Bang Bang controller, also called an on-off controller, which switches rapidly between the maximum and minimum pressure commands, provides a worst-case scenario for evaluating the hydraulic system's response. In this study, it is a feedback controller that takes the slip error signal as input and determines the required brake force to be applied to minimize the slip and avoid locking of wheels [6].

This controller is applied to the previously introduced E-bike model, and the simulation is implemented by using Simulink, as shown in Figure 2.5

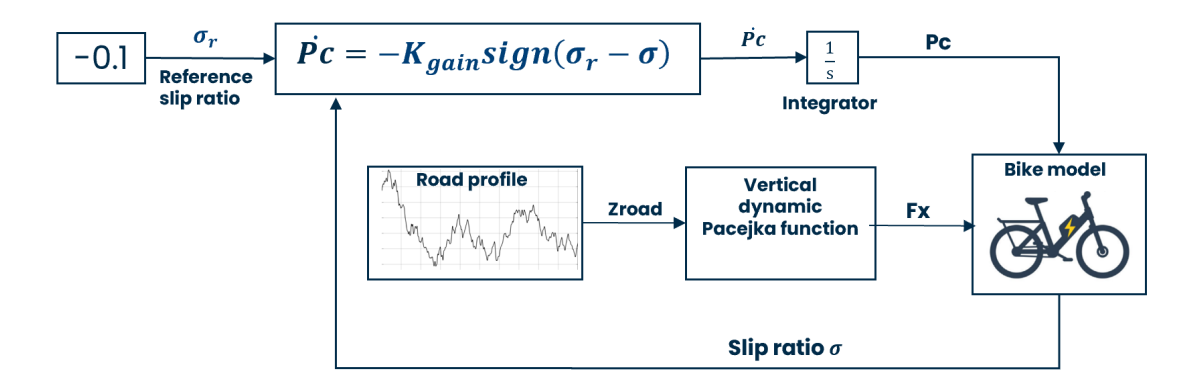


Figure 2.5. Bang-bang controller

First, the optimal slip ratio (reference slip ratio) is set as -0.1 [12]. This value is chosen because it enables the tire to generate the maximum longitudinal braking force, thereby minimizing the braking distance. As shown in the figure 2.6, the longitudinal force reaches the peak values around a slip ratio of -0.1.

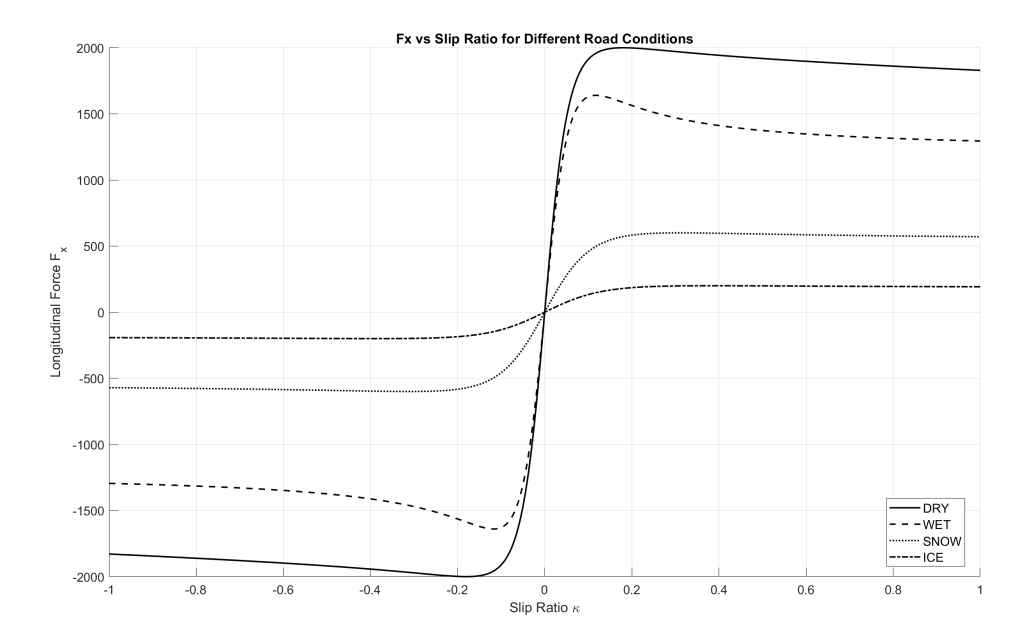


Figure 2.6. Longitudinal force vs. slip ratio [12]

Here is how the Bang Bang controller works:

- If the slip ratio σ is more negative than the reference slip ratio σ_r , the caliper releases pressure, and the controller gain is a positive value.
- If the slip ratio σ is less negative than the reference slip ratio σ_r , the caliper increases pressure, and the controller gain is a negative value.

The controller gain (Variation rate of caliper pressure) is defined as;

$$\dot{P}_c = -K_{gain} \operatorname{sign}(\sigma_r - \sigma) \tag{2.17}$$

Through iterative simulations on a dry road condition, the value of $K_{gain}=110$ bar/s was found to be the minimum rate that produces a consistent and stable limit cycle in the slip ratio. As illustrated in Figure 2.7, the slip ratio oscillates around -0.1, and similar curves can be obtained under other road conditions from Figure 2.9 and Figure 2.11. The simultaneous continuous increase and decrease, from Figure 2.8, Figure 2.10, and Figure 2.12, in caliper pressure also confirms that the ABS is functioning correctly. This value represents a performance threshold; any slower rate would lead to a loss of control and wheel lock-up, while a faster rate, although potentially improving response time, would demand a more powerful and expensive hydraulic actuator.

The selected value of 110 bar/s also fits within the performance range of commercially available, cost-effective hydraulic modulators for two-wheeled vehicles, thus ensuring that the simulation results represent a realistic and feasible system.

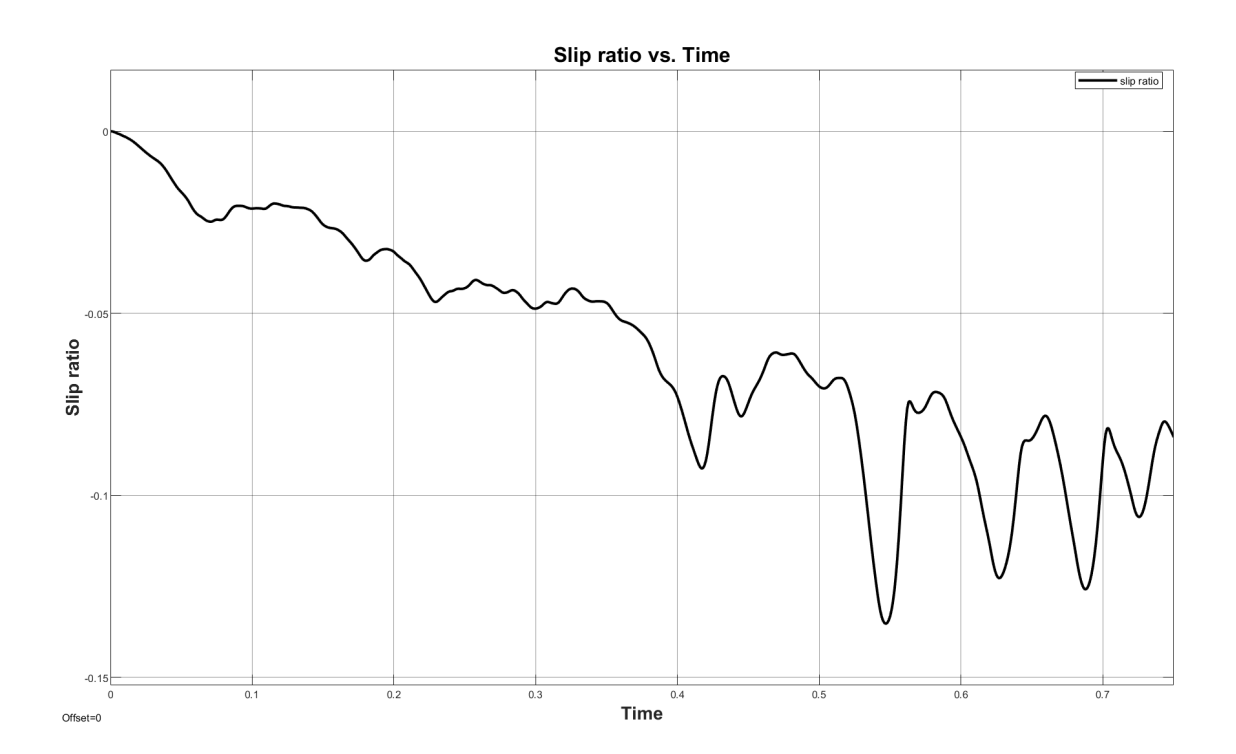


Figure 2.7. Result of the slip ratio on a wet road

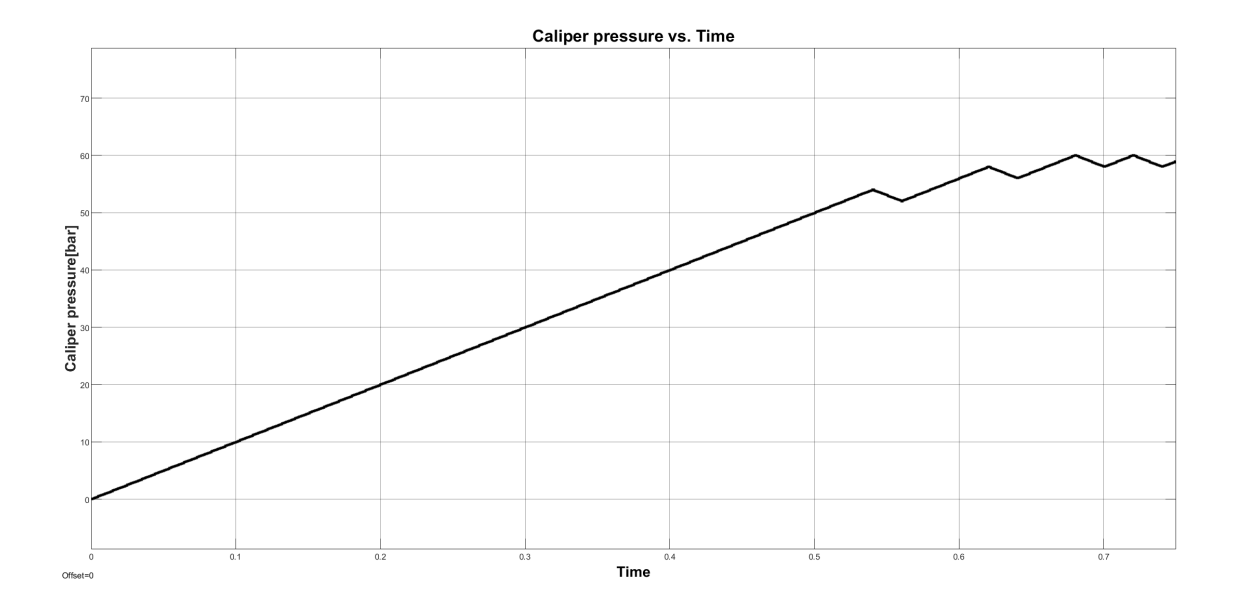


Figure 2.8. Result of the caliper pressure on a wet road

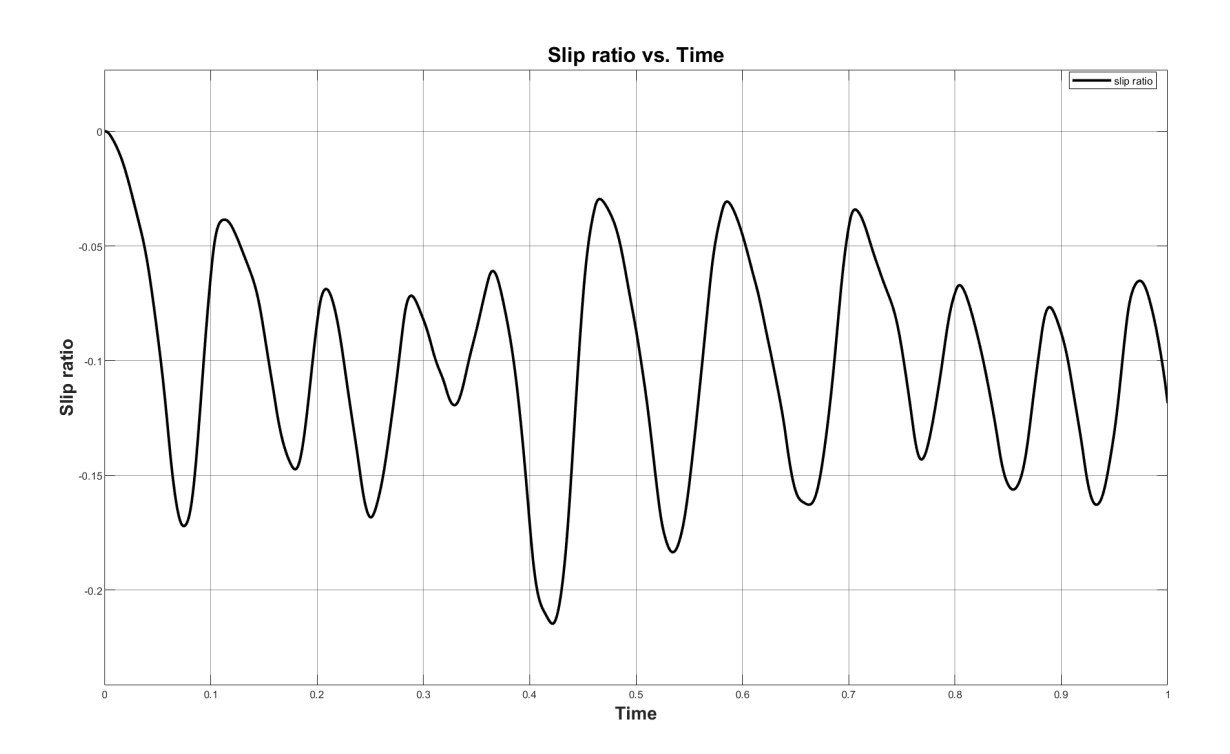


Figure 2.9. Result of the slip ratio on a snow road

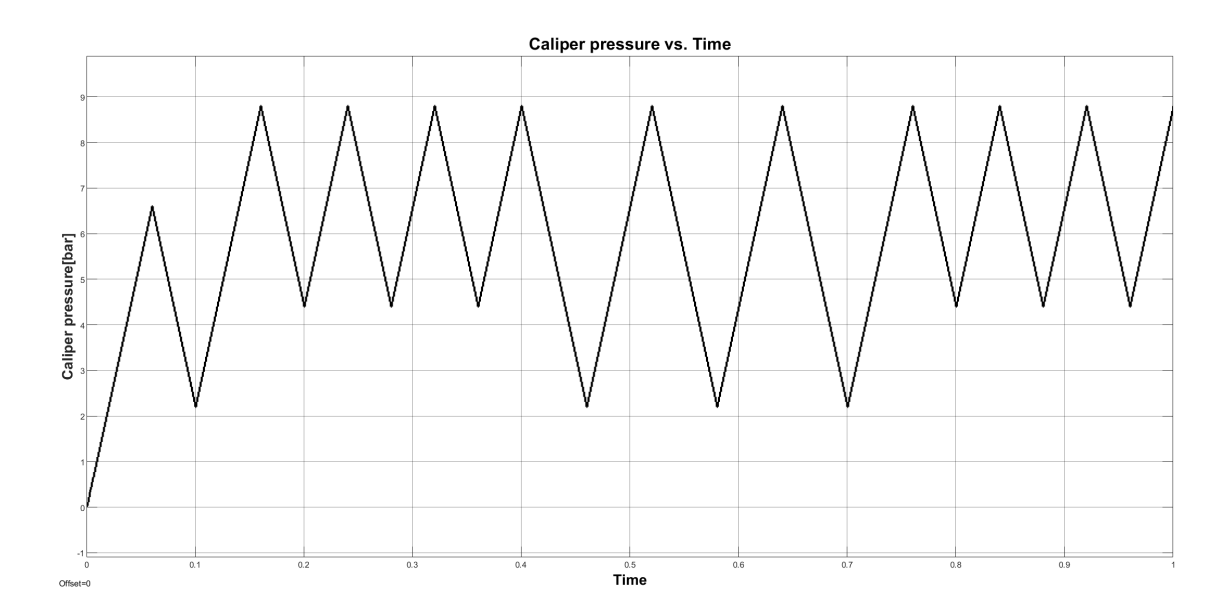


Figure 2.10. Result of the caliper pressure on a snow road

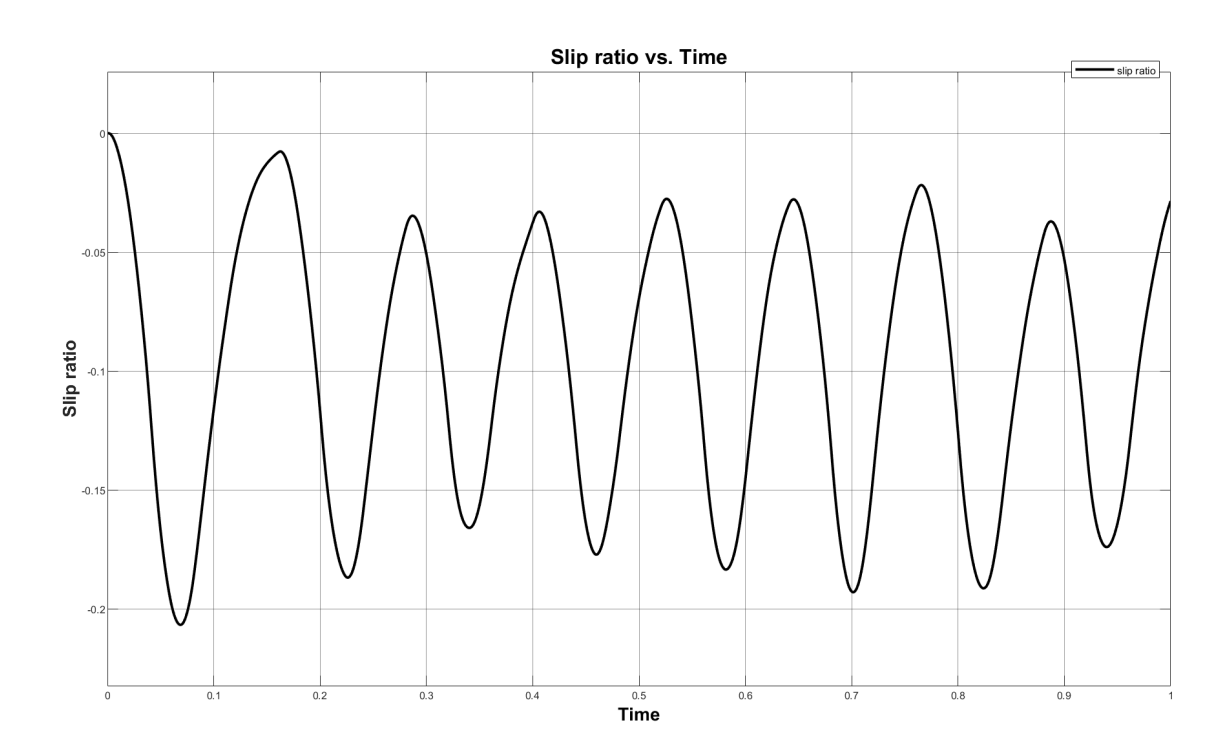


Figure 2.11. Result of the slip ratio on an ice road

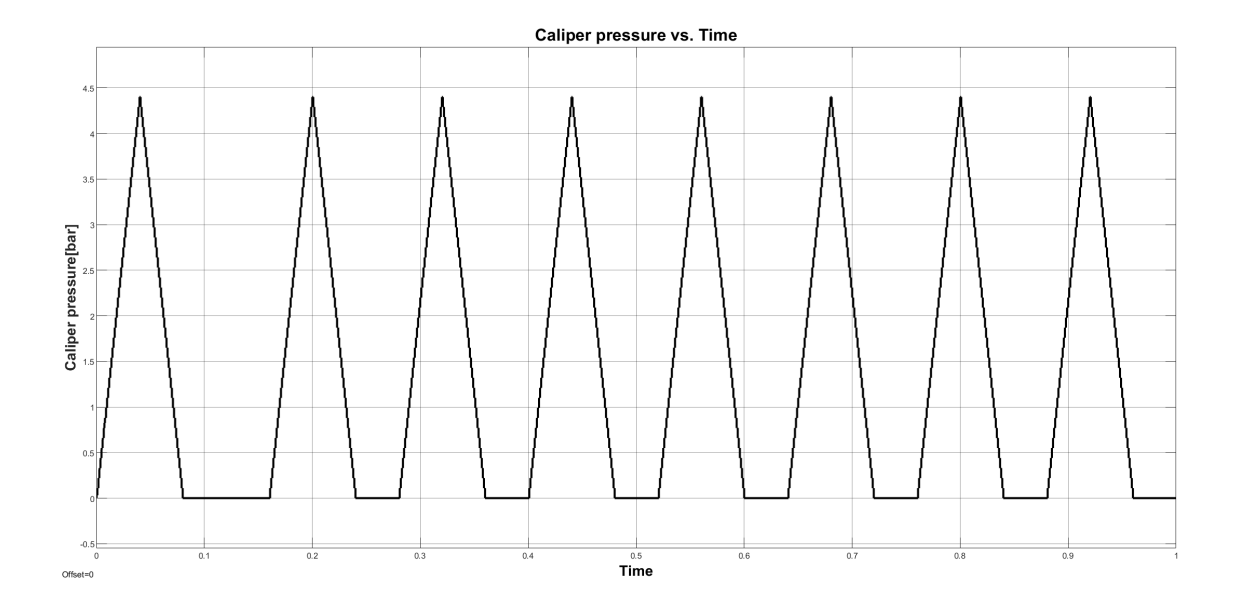


Figure 2.12. Result of the caliper pressure on an ice road

Frequency of the valve switch

In addition, the frequency of hydraulic solenoid valve opening and closing is also one of the important factors affecting the braking. Due to the physical and mechanical structure limitations of the valve, the switch frequency of the valve is not infinitely high. The limitation of hydraulic solenoid valve frequency is generally around 10 - 100 Hz [13]. In this work, the hold valve is normally open while normally braking. Once lock-up is detected, it closes. The closing time is 3 ms, and the frequency f_{val} is chosen as 50 Hz. On the contrary, the Release valve is normally closed while braking. Once lock-up is detected, it opens. The opening time is 1 ms, and the frequency is chosen as 50 Hz. It is important to note that this model assumes an idealized actuator with a fixed pressure change rate and fixed valve switch frequency. The hydraulic system assumes linear, first-order dynamics. In a physical system, solenoid valve delay and hydraulic fluid dynamics would introduce more complex, nonlinear responses. This simplification may lead to an overestimation of the controller's performance in simulation.

2.6 Model limitations and critical analysis

Although the models described above can effectively simulate a vehicle's longitudinal dynamics, it must be acknowledged that they inherently involve simplifications. Moreover, these simplifications may impact the validity of the simulation results. The following section will critically analyse these limitations.

2.6.1 Limitations of the Bike Model

- Single-wheel model: The model reduces the E-bike to a single front wheel, neglecting the dynamics of the rear wheel. Consequently, it cannot simulate pitching motion, rear-wheel lift-off, or the effect of rear-wheel braking. Although the proportion of braking force provided by the rear wheels is relatively small, it still influences the overall longitudinal dynamic characteristics, which have not been considered in this model.
- Pure longitudinal dynamics: This model focuses only on longitudinal motion. It does not consider lateral dynamics such as skidding or rolling motion. In real-world scenarios, rider actions (turning the steering handlebars) or road irregularities introduce lateral forces, resulting in the wheels unable to travel in a perfectly straight line. In future work, a dual-wheel model can be introduced to simulate more complex motions such as skidding and rolling.
- Estimated parameters: The parameters of the model, such as the height of the center of gravity h_G , are based on estimations. In reality, h_G varies with rider weight, posture, and cargo, leading to inaccuracies in the calculation of load transfer ΔF_z , and the total vertical load $F_{z \ total}$ will be different.
- Linear suspension assumption: The suspension system is modeled with linear stiffness K_s and linear viscous damping C_s . Geometric nonlinearities, friction, and tire damping are neglected, which affects the fidelity of the vertical dynamics response.

2.6.2 Limitations of the Tire Model

- Steady-state assumption: The Pacejka Magic Formula is a steady-state model. It computes tire force instantaneously for a given slip ratio, neglecting the transient relaxation length dynamics present in real tires. Although the relaxation length is used to calculate the slip rate, which affects the results of the Pacejka magic formula, this remains an approximation. Consequently, the model may not fully capture the transient response of real tires under all possible braking scenarios, which may lead to differences in simulated controller performance.
- Parameter sensitivity: The model's accuracy is highly dependent on the empirical parameters (B, C, D, E), which were adopted from literature and manually

tuned for general road conditions. These parameters are not specific to a particular tire, and they are assumed to be constant, neglecting their variation with temperature, wear, and aging.

2.6.3 Limitations of the Braking System Model

- Idealized actuator dynamics: The hydraulic modulator is modeled with a fixed pressure variation rate (110 bar/s), a fixed switch frequency(50 Hz), and first-order linear dynamics. The real-world systems exhibit more complex behaviors, including solenoid valve delay, hysteresis phenomena, and nonlinear pressure-flow characteristics, which are not captured.
- Constant master cylinder pressure: The input pressure P_{master} is modeled as a constant step input (e.g., 70 bar). In reality, a rider's braking action builds this pressure over a short but finite time. Although brief, this transient may slightly influence the initial dynamics of the braking event.
- Constant friction coefficient: The coefficient of friction μ between the brake pad and disc is assumed constant. While thermal effects are less severe on E-bikes due to lower speeds compared to motorcycles, some fading with temperature is possible and is not modeled.

2.6.4 Conclusion on Limitations

These limitations do not invalidate the research conclusions but rather define the effective boundaries of the model and control strategy. The model provides a sufficient level of fidelity for its primary purpose: the design and initial validation of a high-performance and low-cost ABS control algorithm. The simplifications were necessary to maintain computational efficiency for ABS design.

Moreover, these limitations clearly outline a road map for future work, highlighting the necessity for validation on physical test platforms. Testing on an actual E-bike will ultimately reveal the implications of these simplifications and close the gap between simulation and reality.

2.7 Model Parameters Summary

 ${\it Table 2.3.} \quad {\it Summary of simulation model parameters and values.}$

Symbol	Description	Value	Unit	Source / Note
Vehicle Para	_	varae		Source / Trote
$\frac{\sqrt{\text{circle 1 are}}}{m}$	Total vehicle mass (rider +	108.8	kg	Estimated
770	bike)	100.0	118	Listinated
a	Acceleration of gravity	9.8	m/s^2	_
$\frac{g}{\lambda}$	Bike front weight distribution	0.375	-	Estimated
m_s	Sprung mass	40.8	kg	Calculated: $m_s =$
1108	Sprang mass	10.0	709	$m * \lambda$
m_u	Unsprung mass	12	kg	Estimated
h_G	Height of center of gravity	1	m	Estimated
L	Wheelbase	1.2	m	Typical e-bike
_	,,, <u>11</u> 6612486			value
$R_{ m wheel}$	Wheel radius	0.3517	m	Measured
J_{ω}	Wheel rotational inertia	0.1570	kgm^2	Calculated: $J \approx$
- w				$m_{\rm wheel}R^2$
M_r	Rolling friction torque	0	Nm	Neglected for sim-
•				plicity
b_r	Axle viscous damping coeffi-	0.001	Nms/rad	Tuned
,	cient		,	
Suspension	& Tire Parameters			
k_s	Suspension spring stiffness	13341	N/m	Tuned from Mo-
			,	torcycle Dynam-
				ics : Cossalter,
				Vittore
c_s	Suspension damping coeffi-	2000	N/(m/s)	Tuned from Mo-
	cient			torcycle Dynam-
				ics : Cossalter,
				Vittore
k_t	Tire vertical stiffness	100e3	N/m	Tuned from Mo-
				torcycle Dynam-
				ics : Cossalter,
				Vittore
c_t	Tire damping coefficient	0	N/(m/s)	Neglected for sim-
				plicity
L_{rel}	Relaxation length	0.001	m	Tuned for stable
				response
	em Parameters	1.10		m 1
\dot{P}_c	Pressure increase/decrease	110	bar/s	Tuned via Bang-
D	rate	0.001		Bang control
B_a	Piston radius	0.034	m	Measured
R_m	Effective brake disc radius	0.086	m	Measured
μ	Pad-disc friction coefficient	0.4	_	Assumed con-
A 7	Number of broke rode 26	0		stant
$N_{\rm pad}$	Number of brake pads	2		
P_{master}	Master cylinder pressure	70	bar	Estimated
f_{val}	Frequency of the valve switch	50	Hz	Tuned from A
				review of one-box
				electro-hydraulic
				braking system

Chapter 3

Numerical evaluation

This chapter introduces the methodology used in ABS design and control strategy, presents the system simulation process in MATLAB, and shows the final results obtained.

3.0.1 Overall control strategy

The objective of this study is to design a high-performance, low-cost ABS for e-bikes. Reduced sensor requirements can effectively lower the cost of ABS. Therefore, this ABS must perform effectively with a limited data supply. The conjugate boundary method is an effective method for controlling braking that relies only on wheel acceleration data. This aligns well with the low-cost objective of this study.

3.1 Methodology

3.1.1 Conjugate boundary method controller design

The Conjugate Boundary Method (CBM) is the key control strategy for implementing the ABS function in this thesis. It can regulate brake pressure by monitoring wheel dynamics (wheel acceleration), without slip ratio measurement.

In the CBM approach, the controller switches states between increasing and releasing brake pressure based on specific boundary conditions derived from the system's dynamic behavior. These specific boundary conditions are defined in the Table 3.1

These conditions are derived from the system's dynamic behavior and are categorized into Prediction (P) boundaries (trigger pressure release) and Reselection (R) boundaries (trigger pressure increase) [8].

The CBM control strategy operates as follows:

- When the pressure-increasing trajectory reaches the P boundary, ABS will release the caliper pressure.
- When the pressure-decreasing trajectory reaches the R boundary, ABS will increase the caliper pressure.

P condition	The conditions to be satisfied
P1	$-\dot{\omega}R > k_1$
P2	$\left \begin{array}{c} -\frac{\dot{\omega}}{\omega} > k_2 \end{array} \right $
P3	$-\ddot{\omega}R > k_1 \text{ and } -\frac{\dot{\omega}}{\omega} > k_2$
R condition	The conditions to be satisfied
R1	when P condition is no longer satisfied
R2	a fixed time delay
R3	$\dot{\omega}R > k_3$
R4	$\ddot{\omega} < 0$
R5	$\ddot{\omega} < 0 \text{ and } \dot{\omega}R < k_5$

Table 3.1. P and R conditions for the Conjugate Boundary Method [8]

These conditions are formulated in terms of wheel acceleration and deceleration thresholds. And they can be combined freely to form various control strategies.

From the available boundary conditions in Table 3.1, the combination of P1, R2, and R3 was selected for this implementation. The resulting control strategy is as follows:

- Pressure release condition (P1): When the wheel deceleration is larger than κ_1 , the caliper pressure is released.
- Pressure increase condition (R2 or R3): If wheel acceleration exceeds a threshold κ_3 , or after a fixed time delay κ_2 from the pressure release, then the caliper pressure will increase again.

The selection of boundary conditions for P1, R2, and R3 represents a deliberate design decision. This approach enhances the robustness and performance of the ABS controller under diverse and adverse road conditions.

Although a simpler strategy using only two conditions (e.g., P1 and R3) is feasible, it has a crucial drawback: its performance is highly sensitive to the accuracy of wheel acceleration measurements and the system model.

The introduction of a fixed time delay (R2) provides a crucial fail-safe mechanism. Consider a scenario on extremely low-grip surfaces, such as ice: following pressure release (triggered by P1), wheel acceleration may be extremely low due to insufficient traction. In such cases, the R3 condition may never be satisfied, because wheel acceleration remains too low. A controller relying solely on R3 would become "locked" in the pressure release state, unable to restore pressure, resulting in complete loss of braking force. The R2 condition effectively resolves this issue. After a predefined time interval, pressure is restored regardless of the current wheel acceleration. This ensures the braking process continues even under the most adverse conditions, guaranteeing a braking force is always applied.

If the control strategy works properly, the state trajectory of Tb-S(Brake torque vs. slip ratio) will stay on the limit cycle(red box line in the figure) to prevent wheel lock-up and maximize braking force, as shown in Figure 3.1

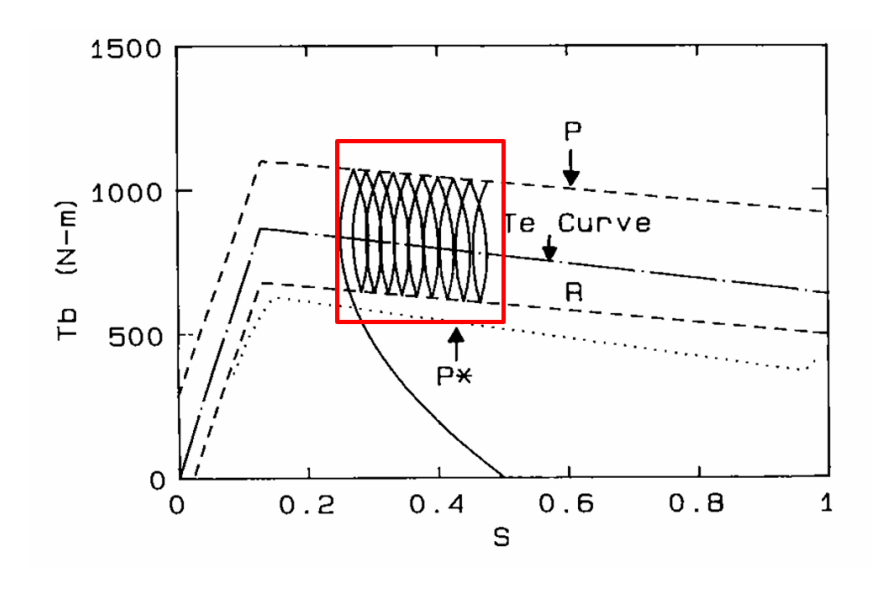


Figure 3.1. Brake torque vs. slip ratio [8]

Ultimately, this control strategy enables the ABS to maintain wheel slip within a desired range without directly measuring the slip ratio, as it only utilizes data on wheel acceleration. These parameters κ_1 , κ_2 , and κ_3 are the most crucial factors for achieving the ABS function, so these should be set properly. However, it is a major challenge to select the optimal values for the parameters due to the complexity of the bike model. Manual tuning is inefficient and impractical. But these parameters do significantly affect braking performance.

To overcome this difficulty, a Genetic Algorithm (GA) is introduced to efficiently search for the global optimal parameter set that minimizes the braking distance.

3.1.2 Parameters optimization via Genetic Algorithm

A genetic algorithm (GA) is an evolutionary optimization algorithm inspired by the principles of natural selection and biological evolution. It simulates the process of survival of the fittest to iteratively search for optimal solutions. The GA is chosen for its ability to efficiently explore complex, non-linear search spaces without requiring gradient information, which is ideal for this tuning problem [9].

The advantages of the GA are not only that it can search for the optimal solution in complex or discontinuous problems, but it is also less prone to falling into a local optimum. Thus, it is a feasible way to find optimal parameters in CBM by using a genetic algorithm.

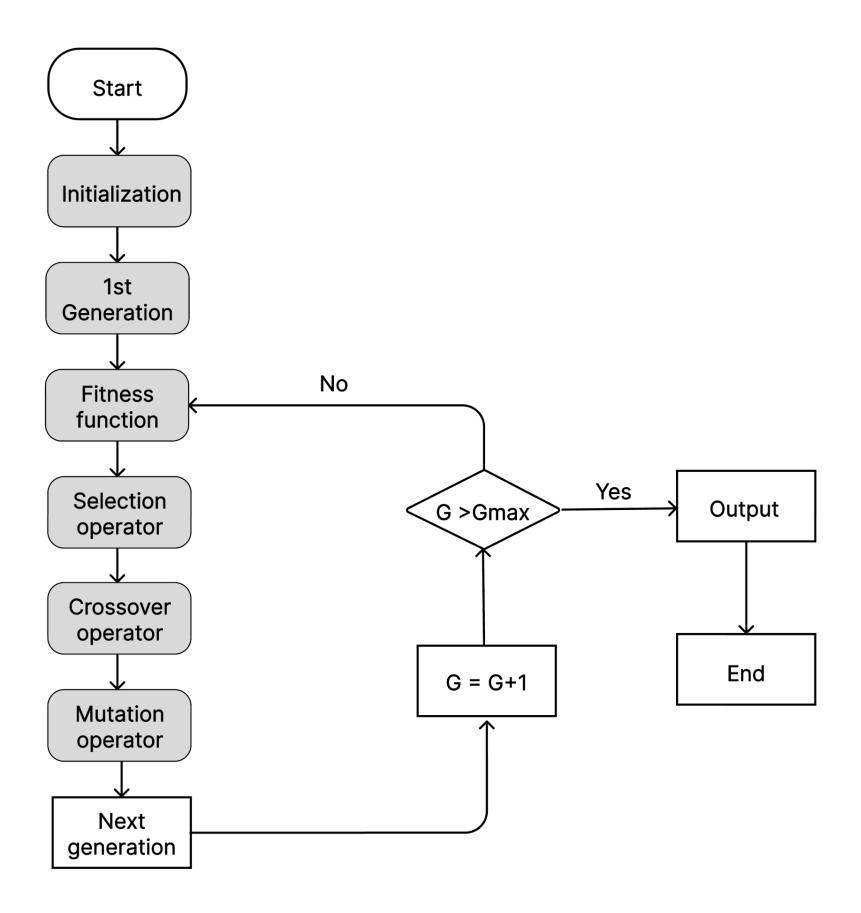


Figure 3.2. Genetic Algorithm iteration process

The main iteration process of the genetic algorithm is shown in Figure 3.2 and Algorithm 1

Initially, the GA randomly selects the candidate parameters from a predefined range as the first generation. And then evaluates them by using an objective function, giving a fitness value (Line 4 in Algorithm 1). For each candidate parameter set, a full braking simulation is executed in the Simulink environment. The braking distance from this simulation is used as the fitness score; a shorter distance corresponds to a higher fitness.

GA will select the results with higher fitness values as the parents. After crossover and mutation operations to avoid falling into a local optimum, GA generates the next generation. By repeating these steps for many iterations until the maximum generations, the GA returns the best individual found throughout the entire process.

Algorithm 1 Genetic Algorithm Optimization Process

Require: Population size, Max generations, Crossover rate, Mutation rate

Ensure: Optimal solution (k_1, k_2, k_3)

- 1: Initialize: Randomly generate the first generation population.
- 2: **for** generation = 1 **to** Max generations **do**
- 3: **for** each individual **in** population **do**
- 4: Run simulation in Simulink > Evaluate fitness (braking distance)
- 5: end for
- 6: **Selection:** Select parents based on fitness (shorter braking distance = higher fitness).
- 7: **Crossover:** Generate offspring by combining the parameters of parents.
- 8: **Mutation:** Perturb offspring parameters with a certain probability.
- 9: Replace the current population with the new offspring to form the next generation.
- 10: end for
- 11: **return** The individual with the highest fitness from all generations.

The performance and convergence of the Genetic Algorithm are highly dependent on the selection of parameters. After conducting preliminary tuning tests, a compromise was reached between performance and simulation computation time. The following parameters were selected for GA in this study:

Table 3.2. Genetic Algorithm parameters used for optimization.

Parameter	Value
Population Size	50
Maximum Generations	30
Crossover Fraction	0.8
Selection Function	Tournament
Mutation Function	Adaptive Feasible

- Population size 50: A population size of 50 provides a good balance between diversity and computational cost. Smaller populations may lack sufficient diversity and converge too early to local optima, but larger populations will significantly increase the computational cost without guaranteeing a proportional improvement in performance.
- Maximum Generations 30: The termination condition is set to 30 iterations. This value is chosen to ensure conclusive convergence, and it provides a safety margin for more complex optimization scenarios.

- Crossover Fraction 0.8: It facilitates the exchange of beneficial parameter combinations within the population, accelerating convergence towards the optimal region of the search space. The remaining 20% of the new population is generated through mutation, which helps maintain diversity and prevents the algorithm from becoming stuck in local minima.
- Selection Function & Mutation Function: The specific implementations of the genetic operators were chosen from the options provided by MATLAB's Global Optimization Toolbox [14].

3.2 Simulation scheme used for GA

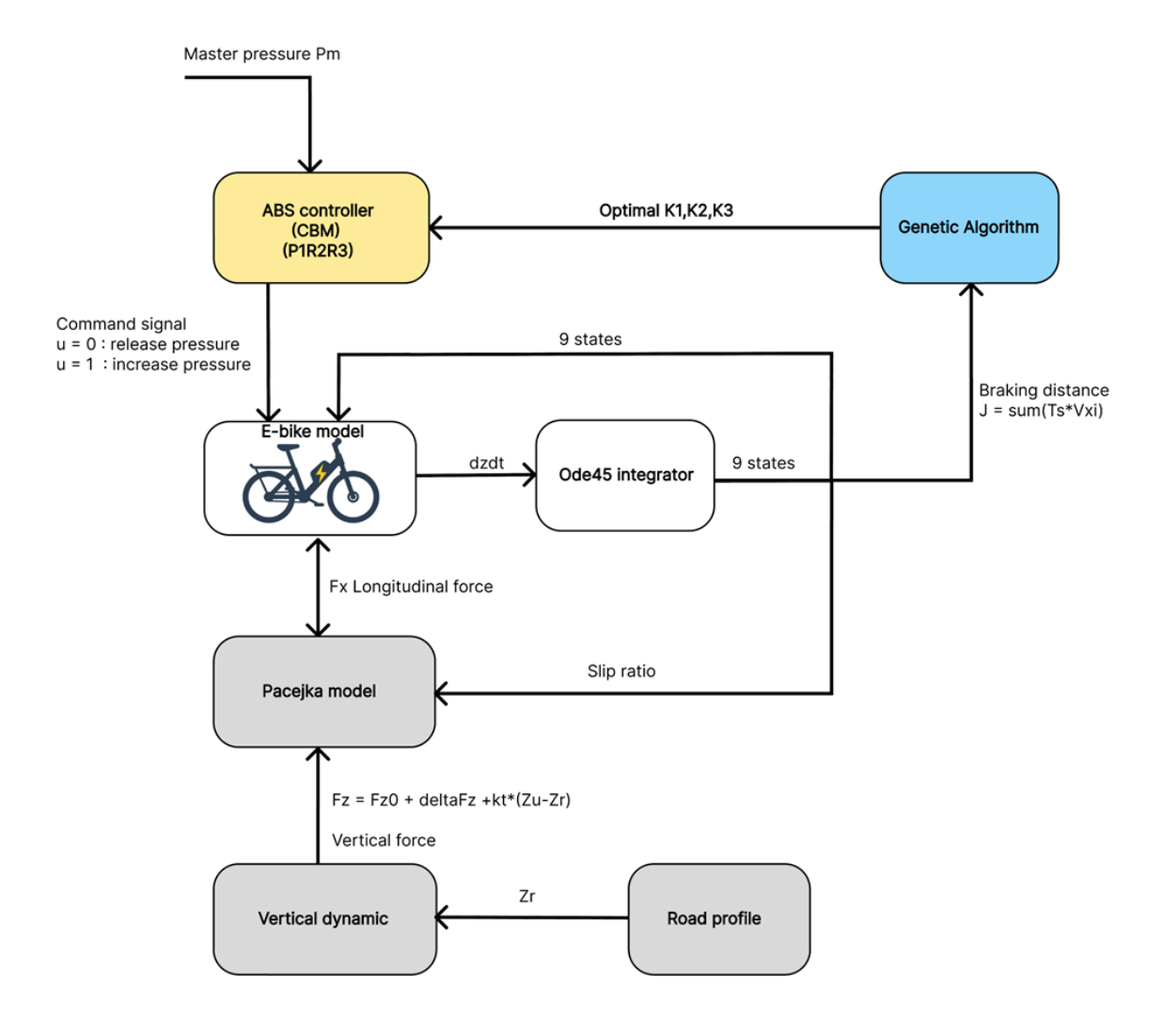


Figure 3.3. Simulation scheme used for GA

Figure 3.3 shows an overview of the braking simulation process, which integrates the Genetic Algorithm optimizer, the E-bike plant model, and ABS controller. This simulation process can be divided into two main phases: the offline parameter optimization loop and the online ABS control loop.

- 1. Offline parameter optimization loop: This phase aims to find the optimal CBM parameters κ_1 κ_2 κ_3 for different road conditions. The road profile Z_r serves as an external input. It is processed by the vertical dynamics model, which calculates the dynamic vertical force F_z acting on the tire. The Pacejka Magic Formula tire model then computes the longitudinal braking force F_x based on the current vertical load and the instantaneous slip ratio κ . The E-bike dynamics model integrates all forces and evolves the system's state variables (e.g., velocity v_x , wheel speed ω , slip ratio κ). The simulation runs until the Bike reaches low speed, and the resulting braking distance is returned to the GA as the fitness value for that parameter set. After evaluating all individuals, the GA performs selection, crossover, and mutation to create a new generation. This loop continues until convergence, and it outputs the optimal parameters.
- 2. Online ABS Control: Once the optimal parameters are found, they are loaded into the CBM controller for performance evaluation. The rider's intent is modeled by applying a step input to the master cylinder pressure. The ABS controller continuously monitors the wheel acceleration. Based only on this acceleration data and the pre-optimized parameters κ_1 κ_2 κ_3 , the CBM determines whether the tires are locked up. The controller then outputs the command signal P_{cCMD} (u = 0/1) to the hydraulic modulator to adjust brake pressure. In the end, prevent lock-up while maintaining maximum braking force.

This integrated framework ensures that the CBM controller is tuned with parameters that are optimal for the entire nonlinear system dynamics.

3.3 Simulation Results

The simulation results presented in this section validate the effectiveness of the Conjugate Boundary Method controller, optimised via a Genetic Algorithm, in preventing wheel lock-up and reducing braking distances across different road conditions. The performance of the designed ABS was evaluated under four distinct road surface conditions: dry, wet, snow, and ice. For each scenario, key state variables including vehicle speed, wheel speed, slip ratio, and caliper pressure were plotted. and compared with the simulation results without ABS. As a result, it proves the controller's capability to maintain optimal braking performance. The results ultimately show that the designed CBM strategy can successfully adapt to varying friction coefficients, ensuring safety and stability during emergency braking.

3.3.1 Dry road simulation result

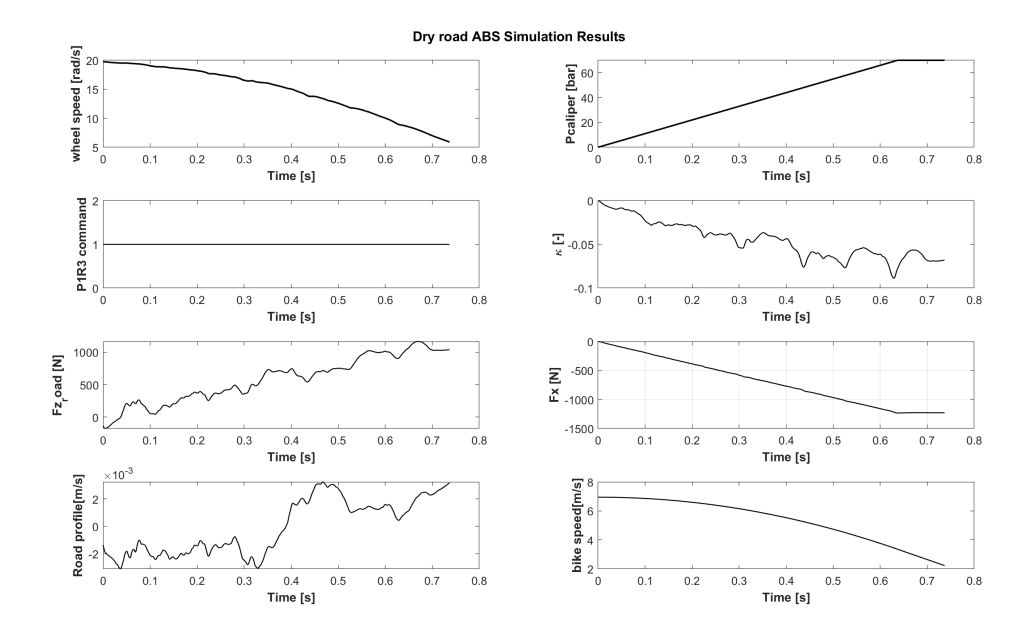


Figure 3.4. Dry road simulation result with ABS on

These diagrams illustrate the results of the simulated E-bike braking on a dry road with ABS. It can be observed that the caliper pressure increases linearly to its maximum value(70 bars), while the wheel speed and bike speed rapidly decrease, and the longitudinal braking force also continuously increases until it reaches a peak of nearly 1200 N. However, ABS was not triggered throughout the entire braking process. And the slip ratio remained above -0.1 throughout the process, indicating that the tires did not lock up.

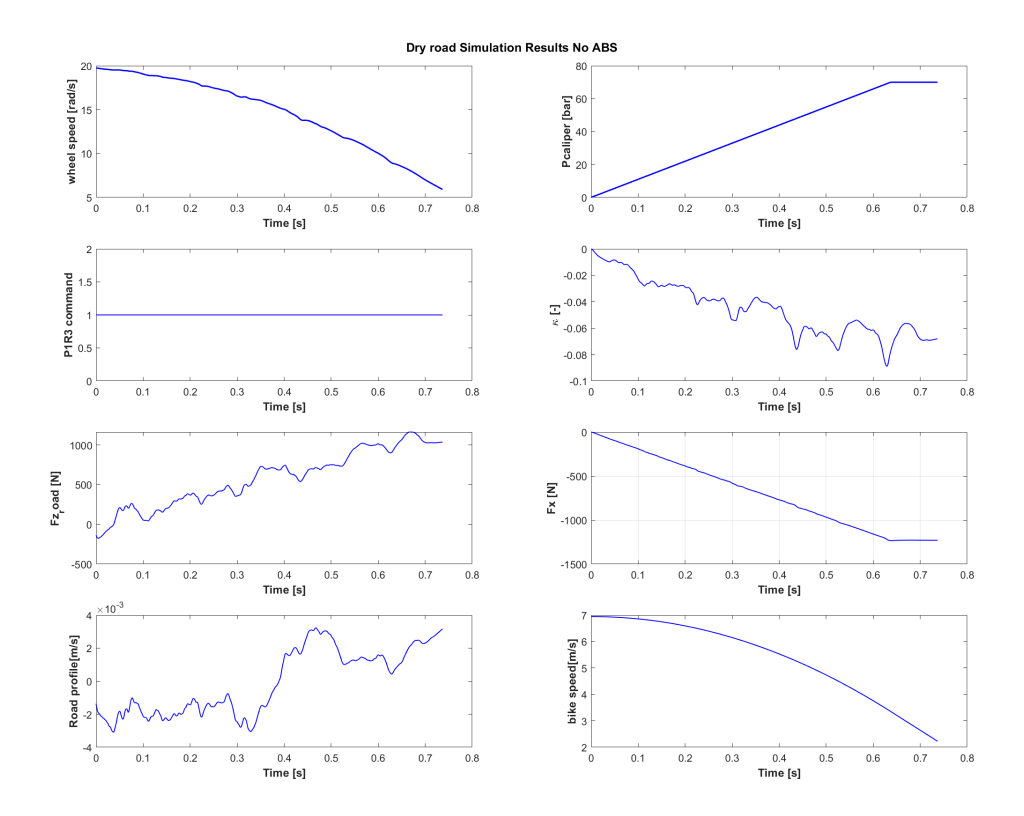


Figure 3.5. Dry road simulation result with ABS off

These diagrams illustrate the results of the simulated E-bike braking on a dry road without ABS. The result is the same as that of the simulation with ABS.

As shown in Figure 3.4, the subplot(P1R3 command Vs time) shows that ABS is not triggered during the entire braking maneuver. This absence of intervention is not a failure of the controller but rather a validation of its correct design logic. On a high-friction surface, such as a dry road, the tire is capable of generating a very high braking force without reaching the critical slip ratio that leads to lockup. As shown in the tire longitudinal force-slip curve (Figure 2.6), the peak friction coefficient is achieved at a slip ratio of approximately -0.1, and the tire can tolerate higher slip values without loss of traction.

In this scenario, the longitudinal braking force generated by the brakes is large (exceeding 1200 N, as shown in the F_x vs time subplot), while the wheel deceleration is significant, it never exceeds the threshold k_1 that triggers the ABS controller to release pressure. The braking torque applied by the calipers remains within the stable range. Consequently, the bike decelerates rapidly and smoothly under purely stable braking conditions. From an initial speed of 25 km/h, the bike decelerates to the preset minimum speed within 1 second.

The fact that the ABS remains inactive on a dry road is a highly desirable outcome. Comparing the results with ABS on and ABS off, the results are exactly the same. It demonstrates that it is unnecessary to introduce ABS for E-bikes during optimal braking conditions. So there are no optimal parameters for CBM.

This also highlights a limitation of the model presented in this paper: it can not consider the motion of rolling over as it utilises a single-wheel model. In reality, if a bike is under such high acceleration, as shown in the Figure 3.4, it is highly probable that the bike will roll over, with the rear wheel losing traction. Due to these limitations, it is necessary to introduce rollover motion into the model in future work.

3.3.2 Wet road simulation result

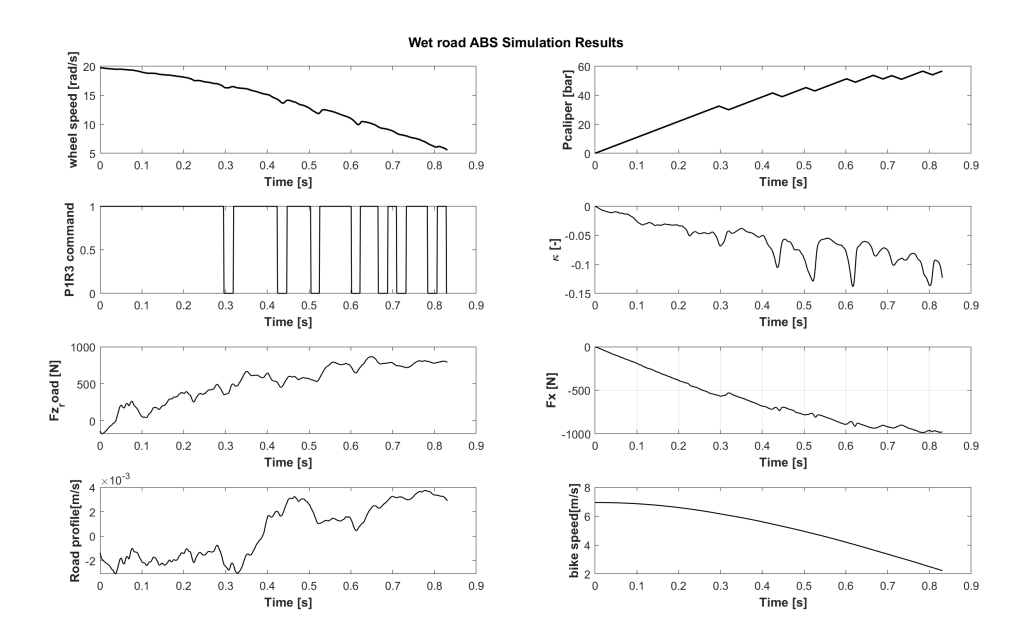


Figure 3.6. Wet road simulation result with ABS on

These diagrams illustrate the results of the simulated E-bike braking on a wet road with ABS. It is clearly observable that the caliper pressure continuously increases and decreases. The ABS command signal also switches between 0 and 1. The longitudinal braking force steadily increased, reaching 1000 N, causing the vehicle speed to decrease rapidly. The slip ratio decreases over time and oscillates around -0.1. These diagrams clearly demonstrate that the ABS is functioning effectively.

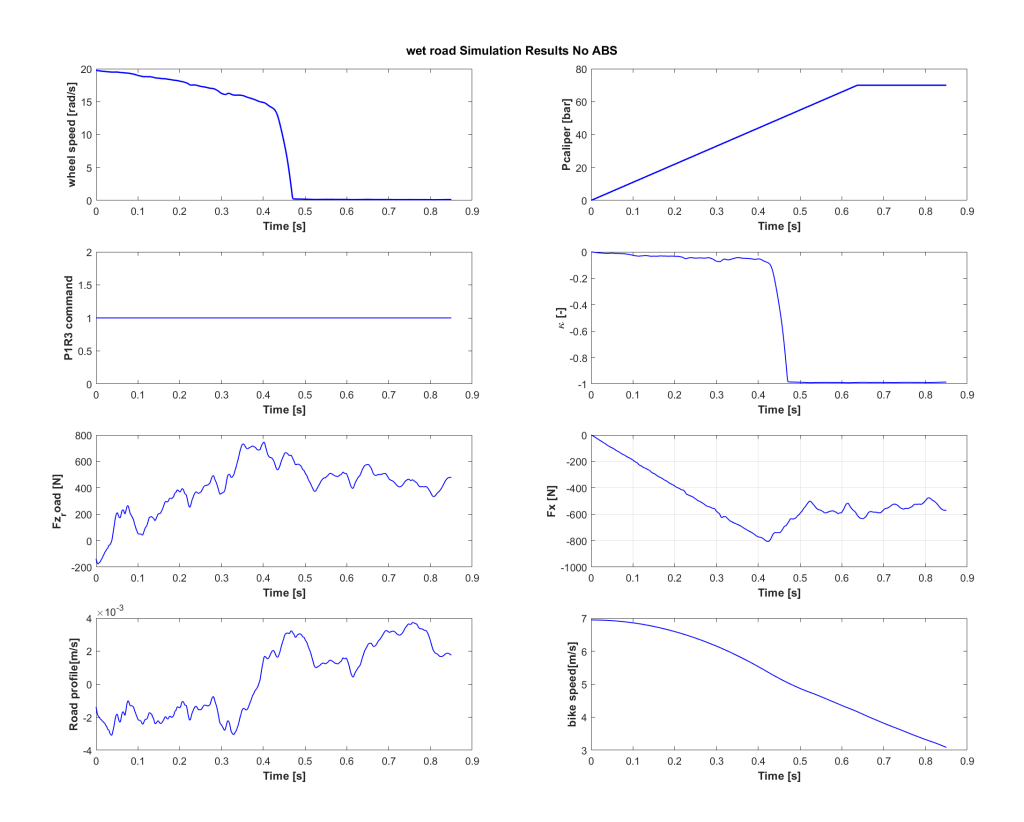


Figure 3.7. Wet road simulation result with ABS off

The results of the simulated E-bike braking on a wet road are totally different without ABS. The wheel speed instantly dropped to zero, with the slip ratio reaching -1, indicating that the wheel had locked up. After wheel lock-up, the longitudinal braking force provided by the tire also decreased from 800 N to less than 600 N. Meanwhile, the rate of decrease in speed has slowed in the bike speed graph.

As shown in Figure 3.6, the simulation results under wet road conditions demonstrate that the ABS functions as intended. The controller command signal alternates between 0 and 1, indicating the system is actively engaged. This enables the slip ratio to oscillate efficiently around -0.1, thereby maintaining the tires near their peak friction limit. Comparing the results of ABS off, the wheels did not lock up. It leads to the longitudinal braking force generated being significantly greater than that produced during wheel lockup. This also leads to higher deceleration and substantially reduced braking distance compared to the ABS off scenario. However, this ideal simulation result must be viewed critically. This model employs a perfectly clean wheel acceleration signal. A real-world sensor includes noise, which may trigger erroneous control actions. Moreover, although braking distances are reduced, high-frequency pressure modulation may induce an uncomfortable pulsing feeling through the brake lever. This phenomenon cannot be

evaluated in simulations but must be considered in actual product design. Therefore, although simulations demonstrate the effectiveness of the control strategy, some ideal assumptions also enhance its performance. A physical test must be required to validate the strategy's robustness under real-world noise and delays in future work.

Finally, the optimal parameters iteratively derived by GA are $k_1=k_3=16.38\,\mathrm{m/s^2}$ $k_2=0.001\,\mathrm{s}.$

3.3.3 Snow road simulation result

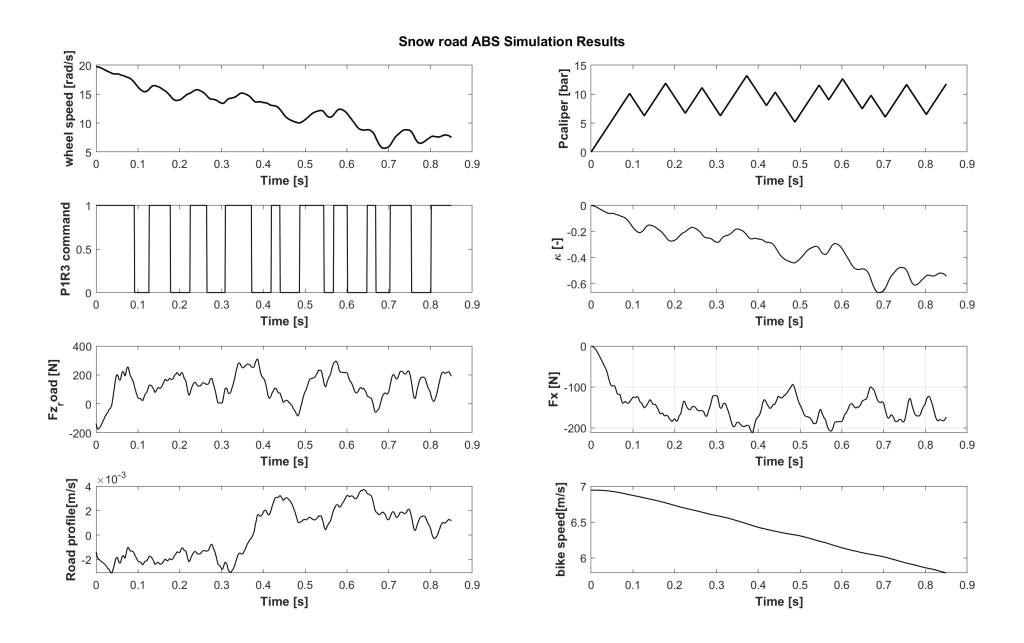


Figure 3.8. Snow road simulation result with ABS on

These diagrams illustrate the results of the simulated E-bike braking on a snow road with ABS. It is clearly seen that compared to the results on the wet road, the wheel speed fluctuations are greater and the ABS control signal frequency is higher. However, the ABS control effectively stabilizes the slip ratio and keeps it away from -1, preventing wheel lock-up.

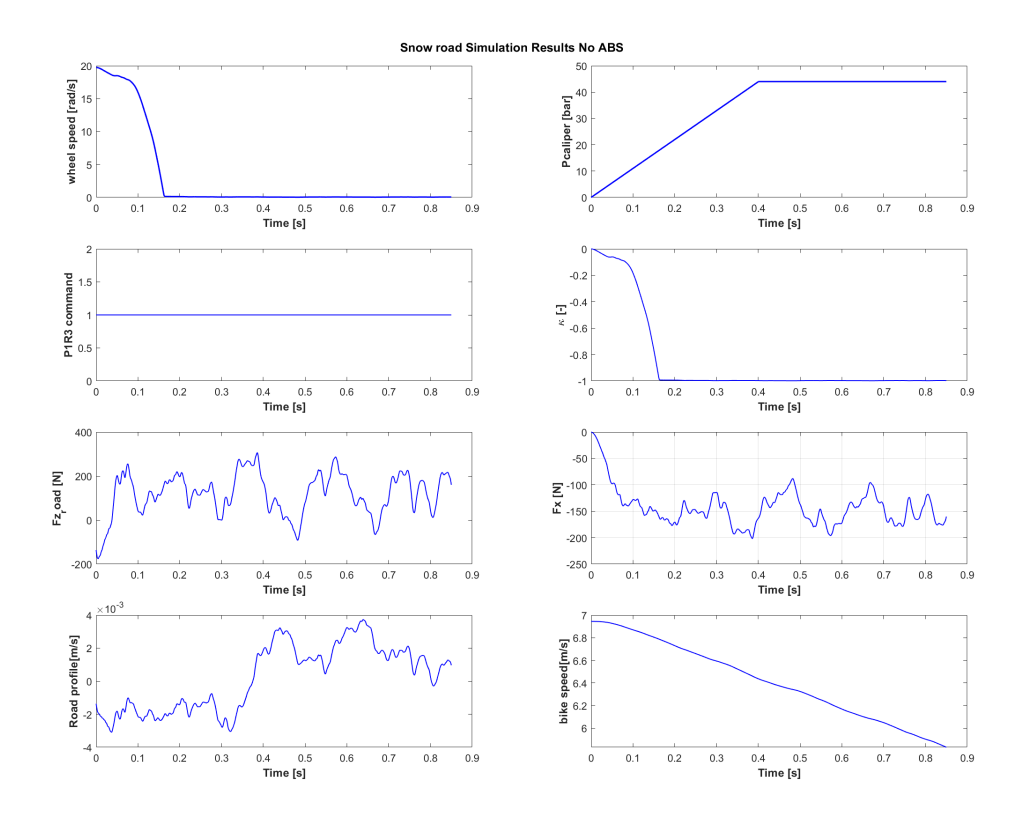


Figure 3.9. Snow road simulation result with ABS off

These diagrams illustrate the results of the simulated E-bike braking on a snow road without ABS. Without a doubt, the wheels locked up, and the slip ratio instantly reached -1. However, the longitudinal braking force is the same as in the ABS simulation.

Simulation results under snowy road conditions indicate that the ABS also functions correctly. The controller command signal alternates between 0 and 1 more frequently, indicating that the system is in an active operational state. It is worth noting that the graph of the longitudinal braking force F_x is exactly the same when the ABS is activated and when it is deactivated. Although longitudinal braking force may not increase when ABS is activated on low-friction surfaces, the crucial difference lies in the bike's lateral stability and steering capability.

With ABS active, the wheels are prevented from fully locking up. This maintained rotation is crucial, as it allows the tires to generate lateral forces in response to steering inputs. Consequently, the rider retains the ability to maneuver and avoid obstacles even during maximum braking, which is a fundamental safety advantage.

Without ABS, the wheels lock up immediately. A locked tire loses its capacity to generate significant lateral forces, effectively rendering the steering mechanism useless. The bike continues on a fixed trajectory dictated by its inertia, regardless of handlebar movement,

increasing the risk of a collision.

Therefore, from this perspective, the primary benefit of the designed ABS on low-friction surfaces is not solely a reduction in braking distance, but more importantly, the preservation of bike control and directional stability.

And finally, the optimal parameters iteratively derived by GA are $k_1=k_3=30.43\,\mathrm{m/s^2}$ $k_2=0.027\,\mathrm{s}.$

3.3.4 Ice road simulation result

Similar to snow roads, an ice road also presents a low-friction surface, with more extreme driving conditions. Even in such an extreme scenario, ABS also functions correctly. The controller command signal alternates between 0 and 1 more frequently, indicating that the system is in an active operational state.

More importantly, the tires did not lock up throughout the process, maintaining vehicle stability and maneuverability. This outcome ultimately demonstrated that even under the most extreme driving conditions, the designed ABS provides a critical safety margin. Even when any braking force is negligible, maintaining control remains essential.

And finally, the optimal parameters iteratively derived by GA are $k_1 = k_3 = 51.59 \,\text{m/s}^2$ $k_2 = 0.056 \,\text{s}$.

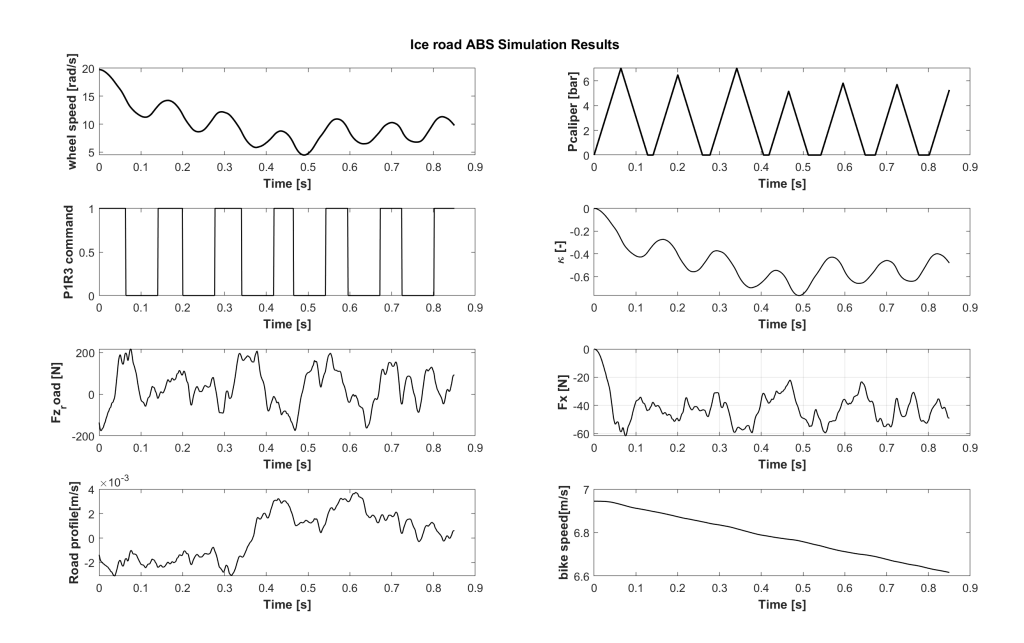


Figure 3.10. Ice road simulation result with ABS on

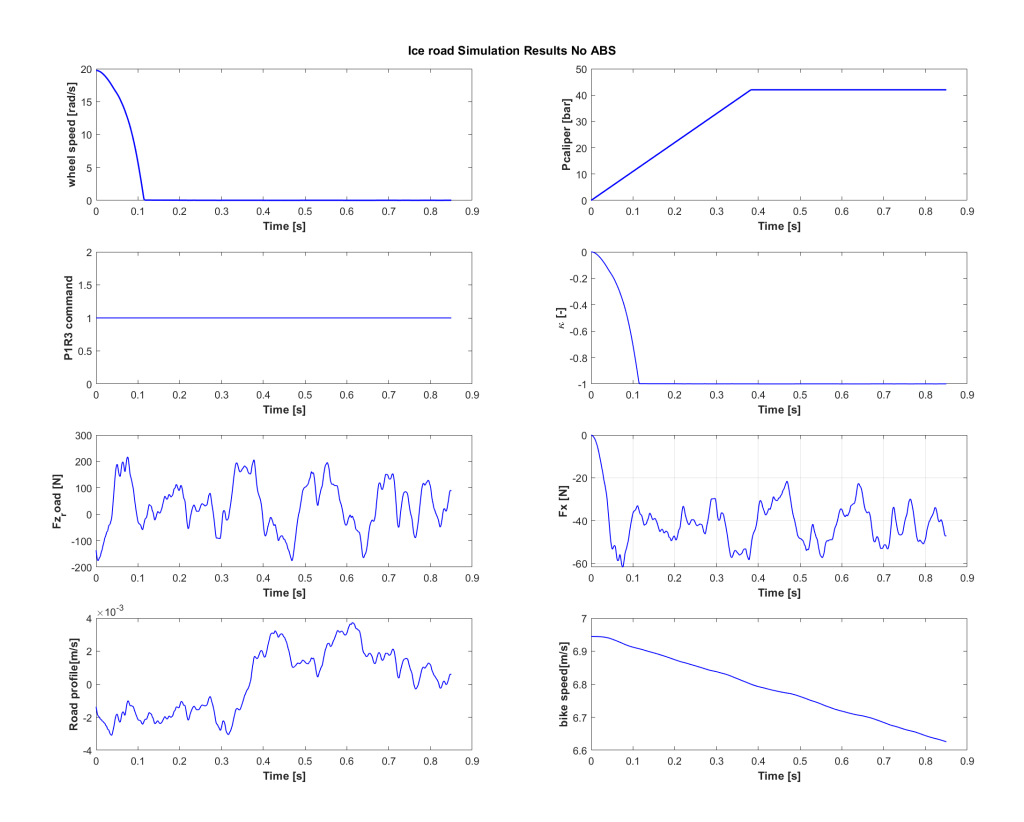


Figure 3.11. Ice road simulation result with ABS off

Additionally, bike braking distance (Obtained by integrating the graph of bike speed versus time) can serve as a key performance indicator (KPI) to demonstrate the effectiveness of the ABS control system. As shown in the table 3.3, in 0.85 seconds of simulated time, on a dry road, the braking distance remains identical with or without ABS, as the ABS has not been triggered. However, on a wet road, the braking distance achieved with ABS is significantly shorter than that without it. Braking distances on snow and ice are also almost the same, but this does not mean ABS is ineffective. As mentioned previously, ABS prevents the slip ratio from reaching -1, thereby preventing wheel lock-up and enhancing the bike's controllability during emergency braking.

Table 3.3. Braking distance under different road conditions with simulation time 0.85s

Road Condition	ABS On [m]	ABS Off [m]	
Dry road	3.94	3.94	
Wet road	4.22	4.50	
Snow road	5.44	5.45	
Ice road	5.49	5.49	

3.3.5 Summary of Results

Finally, the optimal parameters for the Conjugate Boundary Method (CBM), obtained through the Genetic Algorithm optimization process for each road condition, are summarized in Table 3.4. This table serves as a crucial lookup table for implementing an adaptive ABS controller.

The data shows a clear trend: as the road surface friction coefficient decreases, the controller parameters κ_1 , κ_2 , and κ_3 exhibit a monotonically increasing trend. This trend is due to the high tendency for wheel lock-up on low-friction surfaces such as ice roads. Therefore, the controller must be adjusted to operate with lower sensitivity, so it requires a higher κ_1 threshold to trigger pressure release and permit longer pressure recovery times. It means a longer fixed delay κ_2 .

In practical applications, these pre-optimised parameter sets may be stored within the ABS control unit. A road surface condition estimation algorithm can select the appropriate parameter set from this lookup table in real time, thereby enabling the ABS to adjust its control strategy to achieve optimum performance and safety across different road surfaces.

	Dry road	Wet road	Snow road	Ice road
$\kappa_1 \& \kappa_3 \text{ [m/s}^2$	N/A	16.38	30.43	51.59
Fixed time delay [s]	N/A	0.001	0.027	0.056

Table 3.4. Optimal $\kappa_1 \& \kappa_3$ and fixed time delay (κ_2) under different road conditions

Chapter 4

Conclusion

This thesis presents a complete approach for designing an ABS control system for electric bikes using a simulation method in MATLAB. By modeling the E-bike with a longitudinal and vertical dynamic system and incorporating road profile interaction, the proposed model offers a realistic representation of braking behavior under different road conditions. An effective control strategy, the Conjugate Boundary Method (CBM), is implemented to regulate caliper pressure based solely on wheel acceleration, eliminating the need for slip ratio sensors. To optimize the performance of this controller, a Genetic Algorithm (GA) is applied to automatically search for the optimal CBM parameters that minimize braking distance. The simulation results validate the effectiveness of the proposed ABS system, showing reliable control and stable slip ratio regulation across dry, wet, snow, and icy road conditions.

Overall, the method achieves an efficient, sensor-minimal, low-cost, and high-performance ABS solution for electric bikes.

4.0.1 Future work

Despite the successful design of an efficient, low-cost ABS control system for e-bikes in this thesis, the results are based on various assumptions and ideal models. For future work, establishing more complex models that more accurately reflect real-world conditions is essential. The current model assumes an idealized actuator with fixed pressure variation rates. The immediate next step is to replace this model with a high-fidelity representation of the hydraulic system. This includes characterizing and modeling the dynamic response of solenoid valves (including their switching delays and hysteresis), the model of an accumulator, and the restoring phase must also be considered within the hydraulic model. Validating the controller's performance against these real-world dynamics is essential to ensure its robustness and reliability in a physical prototype. In addition, the current bike model is a single-wheel model. The next step will be to extend this model to a two-wheel model to simulate motion states such as pitching and skidding. So, rollover and skidding flags may also be incorporated into the ABS state machine to simulate the bike's motion during braking more realistically, thereby better handling extreme dynamic conditions. This level of control cannot be achieved solely by regulating caliper pressure through k_1 and k_3 . In the end, the proposed ABS control system will be integrated into a real commercial electric bike to enhance performance and safety.

References

- [1] Fortune Business Insights, "Electric bike market size, share & covid-19 impact analysis, by type (cargo, mountain, trekking, and others), by battery type (lead acid, lithium ion, and others), and regional forecast, 2024-2032." https://www.fortunebusinessinsights.com/electric-e-bike-market-102022, July 2023. Accessed: 2025-09-012.
- [2] D. Adminaité-Fodor and G. Jost, "Safer roads, safer cities: How to improve urban road safety in the eu," Tech. Rep. PIN Flash Report 37, European Transport Safety Council (ETSC), Brussels, Belgium, 2019.
- [3] "Single-vehicle accidents of cyclists," tech. rep., German Insurers Accident Research (UDV), Berlin, Germany, 2025. Accessed: 2025-09-09.
- [4] M. Rizzi, J. Strandroth, A. Kullgren, C. Tingvall, and B. Fildes, "Effectiveness of motorcycle antilock braking systems (abs) in reducing crashes: the first cross-national study," *Traffic Injury Prevention*, vol. 16, no. 2, pp. 177–183, 2015.
- [5] E. C. Yeh, G. K. Roan, and I. H. Yun, "Development of an anti-lock brake system for motorcycle," Vehicle System Dynamics: International Journal of Vehicle Mechanics and Mobility, vol. 24, no. 4-5, pp. 427–444, 1995.
- [6] P. Lakhemaru and S. P. Adhikari, "Design and analysis of vehicle anti-lock braking system with fuzzy logic, bang-bang and pid controllers," *Himalayan Journal of Applied Science and Engineering*, 2020. Available online.
- [7] Data Insights Market, "ebike abs analysis 2025 and forecasts 2033: Unveiling growth opportunities," tech. rep., Data Insights Market, 2025. Accessed: 2025-09-09.
- [8] H. G. Yeh and G. M. Bone, "Conjugate boundary method for control law synthesis and evaluation," *IEEE Transactions on Control Systems Technology*, vol. 38, no. 7, pp. 950–959, 1990.
- [9] B. Alhijawi and A. Awajan, "Genetic algorithms: theory, genetic operators, solutions, and applications," *Evolutionary Intelligence*, vol. 17, pp. 1245–1256, 2024.
- [10] International Organization for Standardization, "ISO 8608:2016 Mechanical vibration Road surface profiles Reporting of measured data." https://www.iso.org/standard/71202.html, 2016. Edition 2, confirmed in 2021.
- [11] H. B. Pacejka, *Tyre and Vehicle Dynamics*. Oxford: Butterworth-Heinemann, 2nd ed., 2006.
- [12] V. Cossalter, Motorcycle Dynamics. Springer, 2nd ed., 2006.
- [13] X. Zhao, L. Xiong, G. Zhuo, W. Tian, J. Li, Q. Shu, X. Zhao, and G. Xu, "A review of one-box electro-hydraulic braking system: Architecture, control, and application," *Sustainability*, vol. 16, no. 3, p. 1049, 2024.

[14] The MathWorks, Inc., "Genetic algorithm - matlab ga." https://www.mathworks.com/help/gads/ga.html, 2024. Accessed: 2025-09-12.